OXFORD

Cerebral Cortex, 2022, **32**, 3706–3725
https://doi.org/10.1093/cercor/bhab442
Advance access publication date: 17 January 2022
Original Article

The effective connectivity of the human hippocampal memory system

Edmund T. Rolls[1,2,3], Gustavo Deco[4,5,6], Chu-Chung Huang[7], Jianfeng Feng[2,3]

[1]Oxford Centre for Computational Neuroscience, Oxford, UK,
[2]Department of Computer Science, University of Warwick, Coventry CV4 7AL, UK,
[3]Institute of Science and Technology for Brain Inspired Intelligence, Fudan University, Shanghai 200433, China,
[4]Department of Information and Communication Technologies, Center for Brain and Cognition, Computational Neuroscience Group, Universitat Pompeu Fabra, Barcelona 08018, Spain,
[5]Brain and Cognition, Pompeu Fabra University, Barcelona 08018, Spain,
[6]Institució Catalana de la Recerca i Estudis Avançats (ICREA), Universitat Pompeu Fabra, Barcelona 08010, Spain,
[7]Shanghai Key Laboratory of Brain Functional Genomics (Ministry of Education), School of Psychology and Cognitive Science, East China Normal University, Shanghai 200062, China
*Address correspondence to Professor Edmund T. Rolls, Department of Computer Science, University of Warwick, Coventry CV4 7AL, UK.
Email: Edmund.Rolls@oxcns.org.

Effective connectivity measurements in the human hippocampal memory system based on the resting-state blood oxygenation-level dependent signal were made in 172 participants in the Human Connectome Project to reveal the directionality and strength of the connectivity. A ventral "what" hippocampal stream involves the temporal lobe cortex, perirhinal and parahippocampal TF cortex, and entorhinal cortex. A dorsal "where" hippocampal stream connects parietal cortex with posterior and retrosplenial cingulate cortex, and with parahippocampal TH cortex, which, in turn, project to the presubiculum, which connects to the hippocampus. A third stream involves the orbitofrontal and ventromedial-prefrontal cortex with effective connectivity with the hippocampal, entorhinal, and perirhinal cortex. There is generally stronger forward connectivity to the hippocampus than backward. Thus separate "what," "where," and "reward" streams can converge in the hippocampus, from which back projections return to the sources. However, unlike the simple dual stream hippocampal model, there is a third stream related to reward value; there is some cross-connectivity between these systems before the hippocampus is reached; and the hippocampus has some effective connectivity with earlier stages of processing than the entorhinal cortex and presubiculum. These findings complement diffusion tractography and provide a foundation for new concepts on the operation of the human hippocampal memory system.

Key words: dorsal visual stream; hippocampal effective connectivity; human episodic memory; orbitofrontal cortex; ventral visual stream.

Introduction

A recent anatomical analysis of the direct connections of the human hippocampal memory system using diffusion tractography with 172 participants in the Human Connectome Project (HCP) (Huang, Rolls, Hsu, et al. 2021b) provides evidence that hippocampal connections are much more extensive than in the simple dual stream model, in which ventral cortical processing streams concerned with representations of "what" object or person is present (Kravitz et al. 2013; Rolls 2021b) reach the hippocampus by the perirhinal and then lateral entorhinal cortex; and the dorsal cortical stream concerned with representations of "where" spatial locations or actions (Gallivan and Goodale 2018) are connected via the parahippocampal gyrus and the medial entorhinal cortex with the hippocampus (Van Hoesen 1982; Suzuki and Amaral 1994; Burwell et al. 1995; Burwell 2000; Knierim et al. 2014; Doan et al. 2019). For example, in humans the diffusion tractography provided evidence for direct connections between the hippocampus that bypass the entorhinal cortex to reach the perirhinal and parahippocampal cortex; and for direct hippocampal connections with early sensory cortical areas for vision, touch, and olfaction; and for cross-connections between the "what" and "where" streams in the connectivity before the hippocampus (Huang, Rolls, Hsu, et al. 2021b). The connections were analyzed between the hippocampal system and the 362 cortical areas defined in the HCP atlas (Glasser et al. 2016) and in our modified and extended version of it, HCPex (Huang, Rolls, Feng, et al. 2021a). However, diffusion tractography has limitations, in that it does not provide evidence about the directionality of the connections; it can be difficult to trace pathways that cross each other; and it does not reveal well the connections between the two hemispheres. These connections receive support from a functional connectivity (FC) investigation, but as that is based on the correlations between the blood

Received: September 13, 2021. **Revised:** November 5, 2021. **Accepted:** November 8, 2021

oxygenation-level dependent (BOLD) signals in pairs of brain regions (Ma et al. 2021), that method cannot measure the direction of effects between brain regions. Many of the connections identified with the diffusion tractography in humans are consistent with tract-tracing studies in macaques, as described elsewhere (Huang, Rolls, Hsu, et al. 2021b) and below.

The aim of the research described here is to use an independent method to measure the strength of the connectivity of the human hippocampal system with different brain areas, in which directionality can be measured, and the crossing of pathways is not a problem. The method that we developed for this is a new way of measuring effective connectivity in the brain from the functional magnetic resonance image (fMRI) BOLD signal, which allows the directionality of the connectivity to be measured. A previous version of the algorithm that measured effective connectivity without direction was the starting point (Deco et al. 2019), and this was developed further to enable it to measure the connectivity in each direction, as described in the Methods. As set out in the Discussion, the effective connectivity algorithm does not show that there is a direct connection between a pair of brain regions, but it does show the directed influence of one brain region on another.

The hypotheses that we investigated included whether the hippocampus does have effective connectivity with neocortical areas beyond what might be mediated just through the entorhinal cortex; whether there are interactions of the hippocampus with some early sensory cortical areas and if so in which direction and which early cortical areas; whether there is segregation between a perirhinal cortex "what" stream and a parahippocampal cortex "where" stream; whether the connectivity from neocortical areas to the hippocampus is mainly hierarchical, from stage to stage, as in the dual stream model; and whether there are interactions between the two halves of the brain for this system, as the direct connectivity in humans (in contrast to rodents; Rolls 2018a) of the hippocampus may be somewhat unilateral, and is not well measured by diffusion tractography (Huang, Rolls, Hsu, et al. 2021b).

A highlight of the present investigation is that it was performed in the same participants as those in which the anatomical connections were described (Huang, Rolls, Hsu, et al. 2021b), facilitating direct comparison between the anatomical connections and the effective connectivity. Another highlight of this investigation is the use of data from the HCP, in which evidence is available from more than 170 participants carefully imaged at 7T with a relatively long imaging time. Another highlight is use of the HCP atlas of 360 cortical areas that have been carefully defined using multimodal information, and in which many of the areas have identified functionality (Glasser et al. 2016), which we have extended by including a redefinition of the hippocampus and subiculum, and to which we have added 66 subcortical areas in an extended HCP atlas HCPex (Huang, Rolls, Feng, et al. 2021a; Huang, Rolls, Hsu, et al. 2021b). Another highlight is the use of the new Hopf algorithm described here for measuring effective connectivity that can operate with 360 or more brain areas. We note that the human brain has developed very greatly in a number of key areas even compared to the macaque, including the temporal lobe with semantic representations for language, the parietal and posterior cingulate cortex, and the orbitofrontal and anterior cingulate cortex (Rolls 2016, 2021d). Given that the human hippocampus is essential for memory function (Corkin 2002; Maguire et al. 2016; Clark et al. 2019), and that the connections between brain areas are important in understanding brain computations (Rolls 2021d), it is a high priority to understand human hippocampal system connectivity with all cortical regions, and this is described here.

Methods

Participants and Data Acquisition

Multiband 7T resting-state fMRIs (rs-fMRIs) of 184 individuals were obtained from the publicly available S1200 release (last updated: April 2018) of the HCP (Van Essen et al. 2013). Individual written informed content was obtained from each participant, and the scanning protocol was approved by the Institutional Review Board of Washington University, St. Louis, MO, United States (IRB #201204036).

Multimodal imaging was performed in a Siemens Magnetom 7T Skyra housed at the Center for Magnetic Resonance at the University of Minnesota in Minneapolis. For each participant, a total of four sessions of rs-fMRI were acquired, with oblique axial acquisitions alternated between phase encoding in a posterior-to-anterior (PA) direction in Sessions 1 and 3, and an anterior-to-posterior (AP) phase encoding direction in Sessions 2 and 4. Specifically, each rs-fMRI session was acquired using a multiband gradient-echo EPI imaging sequence. The following parameters were used: TR = 1000 ms, TE = 22.2 ms, flip angle = 45°, field of view = 208 × 208, matrix = 130 × 130, 85 slices, voxel size = 1.6 × 1.6 × 1.6 mm^3, and multiband factor = 5. The total scanning time for each session for the rs-fMRI protocol was approximately 16 min with 900 volumes. The time series used here thus contained 900 data points for every brain region from the first session. Further details of the 7T rs-fMRI acquisition protocols are given in the HCP reference manual (https://humanconnectome.org/storage/app/media/documentation/s1200/HCP_S1200_Release_Reference_Manual.pdf).

This investigation was designed to complement an investigation with diffusion tractography (Huang, Rolls, Hsu, et al. 2021b), and to ensure that the participants were very similar in both investigations, eight rs-fMRI participants were excluded: six with no diffusion scans and two with incomplete rs-fMRI sessions. Then, to allow a comparison of the 7T data described here with results obtained at the 3T rs-fMRI data set, five participants were

excluded: three with no 3T fMRI scans and two with incomplete rs-fMRI sessions. This provided 172 participants for the analyses described here (age 22–36 years, 66 males), each with four sessions of 7T rs-fMRI, of which the first was used for the effective connectivity analysis described here.

Data Preprocessing

The preprocessing was performed by the HCP as described in Glasser et al. (2013), based on the updated 7T data pipeline (v3.21.0, https://github.com/Washington-University/HCPpipelines), including gradient distortion correction, head motion correction, image distortion correction, spatial transformation to the Montreal Neurological Institute space using one-step spline resampling from the original functional images followed by intensity normalization. In addition, the HCP took an approach using ICA (FSL's MELODIC) combined with a more automated component classifier referred to as FIX (FMRIB's ICA-based X-noisifier) to remove non-neural spatiotemporal artifact (Smith et al. 2013; Griffanti et al. 2014; Salimi-Khorshidi et al. 2014). This step also used 24 confound time series derived from the motion estimation (6 rigid-body parameter time series, their backward-looking temporal derivatives, plus all 12 resulting regressors squared (Satterthwaite et al. 2013) to minimize noise in the data. (The mean framewise displacement was 0.083 ± 0.032 std.) The time series were detrended, and temporally filtered with a second-order Butterworth filter set to 0.008–0.08 Hz.

As is evident from the above, the HCP was extremely careful in its preparation of the time series, to minimize any unwanted noise from head motion etc. To address this further, we performed a further analysis with the same 172 participants at 3T that has a 1200 point time series with TR = 0.72. In this set of data, it was possible to regress out the framewise displacement, and it was found that this made little difference, in that the FCs with and without regression of framewise displacement were correlated 0.987. (The FCs are relevant here, because the effective connectivity is calculated using the FCs and the time-lagged FCs.) [Framewise displacement measures the movement of the head from one volume to the next and is calculated as the sum of the absolute values of the six realignment estimates (three translation and three rotation parameters) at every time point (Power et al. 2012).] We also performed cross-validation and showed that the FCs described here for 172 participants at 7T were correlated 0.944 with those in 845 different HCP participants at 3T. These precautions and cross-validation thus show that the connectivity measurements described here are robust. It is also noted that although signal dropout can be a complication of fMRI in the medial temporal lobe, this is unlikely to differentially influence the nine regions of interest (ROIs) analyzed here, as they are all close together in the brain (Fig. 1). Furthermore, we checked the temporal signal-to-noise ratio for all brain regions, and that provided evidence that signal dropout was not a problem.

Brain Atlas and Seed Selection

To construct the effective connectivity for the ROIs in this investigation with other parts of the human brain, we combined the following atlases, as fully described elsewhere to produce the extended HCP atlas HCPex (Huang, Rolls, Feng, et al. 2021a): 1) HCP's multimodal parcellation (v1.0), including 179 cortical regions per hemisphere except for the hippocampus (Glasser et al. 2016); 2) 9 subcortical regions per hemisphere from the CIT168 reinforcement learning atlas (Pauli et al. 2018), including the putamen, caudate nucleus, nucleus accumbens, globus pallidus externalis, globus pallidus internalis, substantia nigra pars compacta, substantia nigra pars reticulata, ventral tegmental area, and mammillary bodies; 3) the thalamic nuclei as described in Iglesias et al. (2018). These atlases are defined in the asymmetric MNI space of ICBM152 2009c (Fonov et al. 2011). To distinguish the subiculum from the hippocampus, we used the subiculum mask provided in the CoBrALab atlas (Winterburn et al. 2013). The amygdala came from the same atlas. Thus, the final modified HCP atlas contained 362 parcels that cover the cerebral cortex. A list of these regions is provided in Supplementary Table 1, and coronal slices with the HCP parcellation with labels for each region are provided in Supplementary Figure 1 with a more extensive series elsewhere (Huang, Rolls, Feng, et al. 2021a). The HCPex atlas is in volumetric space, partly because this facilitates inclusion of subcortical areas, and partly because this allows the use of much software that performs analyses in volumetric MNI space (Huang, Rolls, Feng, et al. 2021a). We note that analyses in surface space are likely to have some advantages for cortical areas because of better registration (Coalson et al. 2018; Huang, Rolls, Feng, et al. 2021a), so we checked whether the volumetric HCPex atlas was accurate for the present purposes. We found that for the 360 cortical areas in the surface-based HCP-MMP v1.0 atlas (Glasser et al. 2016), the correlation of the FCs averaged over 171 participants at 7T with those calculated with the HCPex volumetric atlas (Huang, Rolls, Feng, et al. 2021a) and used here was 0.94, and regard that as satisfactory for the present purposes. (It is this FC matrix and its time-lagged version averaged across participants, which are used by the effective connectivity algorithm described here.)

In this investigation, the same nine seed ROIs were included as in the complementary diffusion tractography investigation (Huang, Rolls, Hsu, et al. 2021b) to investigate their whole-brain FCs. They were the hippocampus (Hipp), subiculum (Subic), presubiculum (PreS), entorhinal Cortex (EC), perirhinal cortex (PeEc), and parahippocampal gyrus (area TF; area TH in terms of three subregions PHA1–3), as shown in Figure 1. Of the four parahippocampal areas, PHA1–3 correspond to area TH (which is medial to and extends posterior to area TF), where within TH, PHA1 is medial, PHA2 is dorsolateral, and PHA3 is

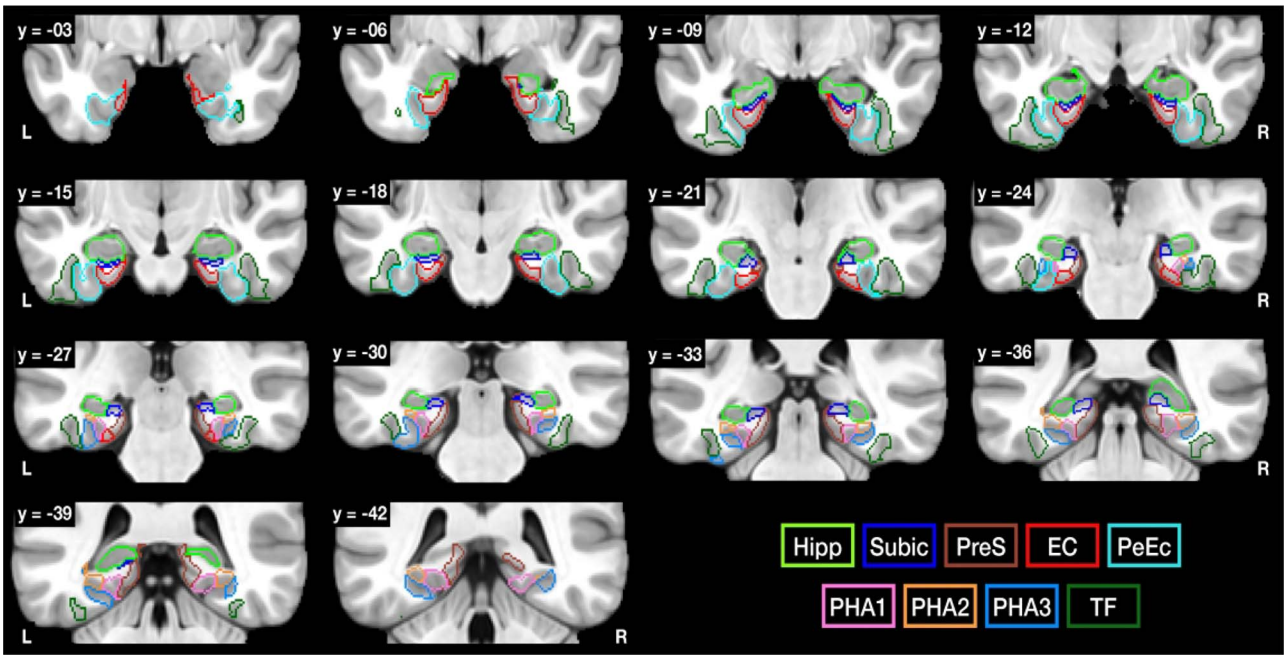

Fig. 1. The hippocampal, parahippocampal, and related ROIs as defined in the HCP atlas (Glasser et al. 2016) that were used for the functional connectivity. EC, entorhinal cortex; Hipp, hippocampus; PeEc, perirhinal cortex; PHA1–3, parahippocampal gyrus areas 1–3; TF, parahippocampal area TF; PreS, presubiculum; Subic, subiculum. For the hippocampus and subiculum, the templates were from Winterburn et al. (2013). The y values of these coronal slices are in MNI coordinates. R indicates right hemisphere.

ventrolateral (see Fig. 1) (The hippocampus defined in this investigation was slightly larger than in the original HCP atlas [Glasser et al. 2016] and was separated from the subiculum, as described in the Supplementary Material.)

Measurement of Effective Connectivity

Effective connectivity measures the effect of one brain region on another and utilizes differences detected at different times in the signals in each connected pair of brain regions to infer effects of one brain region on another. One such approach is dynamic causal modeling, but it applies most easily to activation studies and is typically limited to measuring the effective connectivity between just a few brain areas (Friston 2009; Valdes-Sosa et al. 2011; Bajaj et al. 2016), though there have been moves to extend it to resting-state studies and more brain areas (Frassle et al. 2017; Razi et al. 2017). The method used here was developed from a Hopf algorithm to enable measurement of effective connectivity between many brain areas, described by Deco et al. (2019). A principle is that the FC is measured at time t and time $t+$ tau, where tau is typically 2 s to take into account the time within which a change in the BOLD signal can occur, and then the effective connectivity model is trained by error correction until it can generate the FC matrices at time t and time $t+$ tau. Further details of the algorithm, and the development that enabled it to measure the effective connectivity in each direction, are described next and in more detail in the Supplementary Material.

To infer the effective connectivity, we use a whole-brain model that allows us to simulate the BOLD activity across all brain regions and time. We use the so-called Hopf computational model, which integrates the dynamics of Stuart–Landau oscillators, expressing the activity of each brain region, by the underlying anatomical connectivity (Deco, Kringelbach, et al. 2017b). As mentioned above, we include 362 cortical brain areas in the model (Huang, Rolls, Feng, et al. 2021a). The local dynamics of each brain area (node) is given by Stuart–Landau oscillators which expresses the normal form of a supercritical Hopf bifurcation, describing the transition from noisy to oscillatory dynamics (Kuznetsov 2013). During the last years, numerous studies were able to show how the Hopf whole-brain model successfully simulates empirical electrophysiology (Freyer et al. 2011, 2012), MEG (Deco, Cabral, et al. 2017a), and fMRI (Kringelbach et al. 2015; Deco, Kringelbach, et al. 2017b; Kringelbach and Deco 2020).

The Hopf whole-brain model can be expressed mathematically as follows:

$$\frac{dx_i}{dt} = \overbrace{\left[a_i - x_i^2 - y_i^2\right]x_i - \omega_i y_i}^{\text{Local Dynamics}} + \overbrace{G\sum_{j=1}^{N} C_{ij}\left(x_j - x_i\right)}^{\text{Coupling}} + \overbrace{\beta\eta_i(t)}^{\text{Gaussian Noise}}, \quad (1)$$

$$\frac{dy_i}{dt} = \left[a_i - x_i^2 - y_i^2\right]y_i + \omega_i x_i + G\sum_{j=1}^{N} C_{ij}\left(y_j - y_i\right) + \beta\eta_i(t). \quad (2)$$

Equations (1) and (2) describe the coupling of Stuart–Landau oscillators through an effective connectivity matrix C. The $x_i(t)$ term represents the simulated BOLD signal data of brain area i. The values of $y_i(t)$ are relevant to the dynamics of the system but are not part of the information read out from the system. In these

equations, $\eta_i(t)$ provides the additive Gaussian noise with standard deviation β. The Stuart–Landau oscillators for each brain area i express a Hopf normal form that has a supercritical bifurcation at $a_i = 0$, so that if $a_i > 0$ the system has a stable limit cycle with frequency $f_i = \omega_i/2\pi$ (where ω_i is the angular velocity); and when $a_i < 0$ the system has a stable fixed point representing a low-activity noisy state. The intrinsic frequency f_i of each Stuart–Landau oscillator corresponding to a brain area is in the 0.008–0.08 Hz band ($i = 1, \ldots, 362$). The intrinsic frequencies are fitted from the data, as given by the averaged peak frequency of the narrowband BOLD signals of each brain region. The coupling term representing the input received in node i from every other node j, is weighted by the corresponding effective connectivity C_{ij}. The coupling is the canonical diffusive coupling, which approximates the simplest (linear) part of a general coupling function. G denotes the global coupling weight, scaling equally the total input received in each brain area. Although the oscillators are weakly coupled, the periodic orbit of the uncoupled oscillators is preserved. Details are provided in the Supplementary Material.

The effective connectivity matrix can be derived by optimizing the conductivity of each existing anatomical connection as specified by the structural connectivity matrix (measured with tractography; Huang, Rolls, Hsu, et al. 2021b) to fit the empirical FC pairs and the lagged FC^{tau} pairs. By this, we are able to infer a nonsymmetric effective connectivity matrix (see Gilson et al. 2016). Note that FC^{tau}, that is, the lagged FC between pairs, lagged at *tau* s, breaks the symmetry and thus is fundamental for our purpose. Specifically, we compute the distance between the model FC simulated from the current estimate of the effective connectivity and the empirical data FC^{emp}, as well as the simulated model FC^{tau} and empirical data FC^{tau_emp} and adjust each effective connection (entry in the effective connectivity matrix) separately with a gradient-descent approach. The model is run repeatedly with the updated effective connectivity until the fit converges toward a stable value.

We start with the anatomical connection matrix C obtained with probabilistic tractography from dMRI (or with a C matrix initialized to zero as described in the Supplementary Material, which in fact was used here because it does not rely on knowledge of the anatomical connections) and use the following procedure to update each entry C_{ij}in the effective connectivity matrix

$$C_{ij} = C_{ij} + \varepsilon\left(FC_{ij}^{emp} - FC_{ij} + FC_{ij}^{tau\_emp} - FC_{ij}^{tau}\right), \quad (3)$$

where ϵ is a learning rate constant, and i and j are the nodes. When updating each connection if the initial matrix is a dMRI structural connection matrix (see Supplementary Material), the corresponding link to the same brain region in the opposite hemisphere is also updated, as contralateral connections are not revealed well by dMRI. The convergence of the algorithm is illustrated in Supplementary Figure 6, and the utility of the algorithm was validated as described below.

For the implementation, we set tau to be 2 s, selecting the appropriate number of TRs to achieve this.

Effective Connectome

Whole-brain effective connectivity (EC) analysis was performed between the nine seed regions, shown in Figure 1, and the 362 regions defined in the modified HCP atlas are shown in Supplementary Table 1 (Huang, Rolls, Feng, et al. 2021a). This EC was computed from the FC and FC^{tau} averaged across all 172 participants. The effective connectivity algorithm was run until it had reached the maximal value for the correspondence between the simulated and empirical FC matrices at time t and $t+$ tau, which was indicated by a minimal mean square error, and maximum correlation between the simulated and empirical FC and FC^{tau} (see Supplementary Material). This analysis utilized the gray matter atlas defined in asymmetric MNI space of ICBM152 2009c (Fonov et al. 2011); download link for this atlas: http://www.bic.mni.mcgill.ca/ServicesAtlases/ICBM152NLin2009), in a modified and extended form (Huang, Rolls, Feng, et al. 2021a).

The effective connectivity calculated between the 362 cortical areas was checked and validated in a number of ways. First, in all cases the 362×362 effective connectivity matrix could be used to generate by simulation 362×362 FC matrices for time t and time $t+$ tau that were correlated 0.8 or more with the empirically measured FC matrices at time t and time $t+$ tau using fMRI. Second, the effective connectivity matrices were robust with respect to the number of participants, in that when the 172 participants were separated into two groups of 86, the correlation between the effective connectivities measured for each group independently was 0.98. Third, the effective connectivities for early visual areas V1, V2, V3, and V4 were compared with the known connections for forward and backward connections involving these areas in macaques (Markov, Vezoli, et al. 2014b), and the human effective connectivity was consistent with the connections in this hierarchically organized system in macaques, with these results shown in Supplementary Figure 5 and described in the Supplementary Material.

Results

Effective Connectivity of the Nine Hippocampal System ROIs with all Cortical Areas

The effective connectivities to the hippocampal system from other cortical areas are shown in Figure 2. The effective connectivities from the hippocampal system to other brain areas are shown in Figure 3. Figures 2 and 3, Supplementary Figures 3 and 4 focus on effective connectivities in the left hemisphere to or from cortical regions in both hemispheres. The left hemisphere was

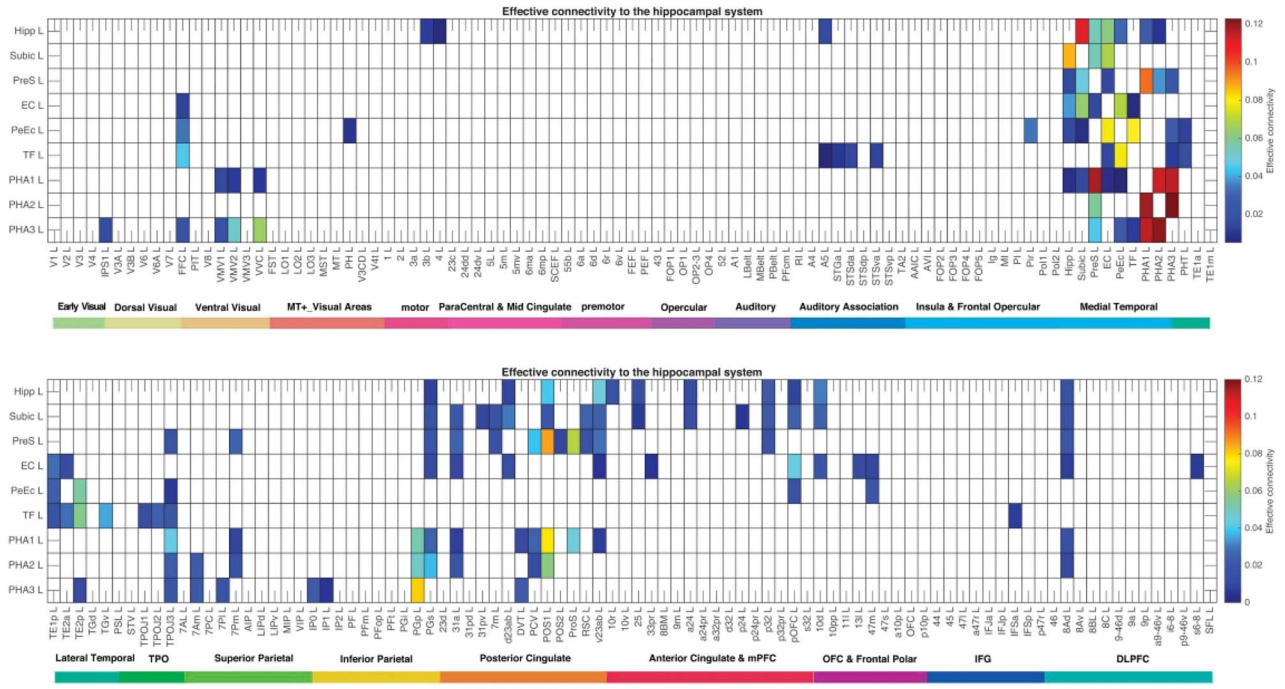

Fig. 2. Effective connectivity to the hippocampal system from all cortical areas in the left (L) hemisphere. The effective connectivity is read from a column to a row. This is calculated from 172 participants in the HCP imaged at 7T. The threshold value for the effective connectivity is 0.005, with a blank indicating effective connectivity less than this, and typically 0. Hipp, hippocampus; Subic, subiculum; PreS, presubiculum; EC, entorhinal cortex; PeEc, perirhinal cortex; TF, parahippocampal area TF; PHA1–3, parahippocampal gyrus TH areas 1–3. The abbreviations for the other brain areas are shown in Supplementary Table 1, and the brain regions are shown in Supplementary Fig. 1. The effective connectivity from the first set of cortical areas is shown above with the subiculum added; and from the second set of areas below.

chosen for these figures to make it likely that any connectivities with language-related areas would be evident. The effective connectivities shown are those calculated over 172 participants with data at 7T in the HCP. In the following sections, the connectivities for each of the hippocampal system areas are considered. A list of the brain regions from the HCP atlas (Glasser et al. 2016) reordered (Huang, Rolls, Feng, et al. 2021a; Huang, Rolls, Hsu, et al. 2021b) is provided in Supplementary Table 1, and coronal slices of the human brain showing where each cortical region is located are provided in Supplementary Figure 1. There are 362 cortical areas in the HCPex atlas used, so the brain regions shown in Figures 2 and 3 as having connectivity with the hippocampus are a small proportion of all these cortical areas. Figures 2 and 3 show that the binary sparseness of the connectivity from the hippocampus to all cortical areas in the left hemisphere = 0.056; and that the binary sparseness of connectivity to the hippocampus from all areas in the left hemisphere is 0.097. (The binary sparseness measures the proportion of effective connectivity links that are not zero.) The sparseness of the effective connectivity matrix across the whole 362 × 362 cortical areas was 0.11. Figures 2 and 3 are helpful because they allow direct comparison with the connections of the human hippocampus traced with diffusion tractography (Huang, Rolls, Hsu, et al. 2021b). Figure 5 provides an overview of some of the effective connectivities to be described.

Hippocampus

The effective connectivity to the hippocampus from other brain areas (Figs 2 and 4) shows that it receives strong-to-moderate influences from the entorhinal cortex, perirhinal cortex, subiculum, presubiculum, parahippocampal gyrus TH, posterior cingulate cortex (v23ab), and an early visual area POS1. Weaker inputs to the hippocampus are directed from the anterior cingulate cortex (p32, a24, 25), orbitofrontal cortex (pOFC and 47m), and prefrontal areas 10d (frontal pole) and 8Ad (dorsolateral prefrontal cortex), somatosensory cortex (3b), and auditory cortex (A5). Some of this connectivity is bilateral as shown below.

Figures 3 and 5 show that the hippocampus has effective connectivity directed strongly to the subiculum and entorhinal cortex; with some effective connectivity to A5, presubiculum, perirhinal cortex, parahippocampal cortex TH (PHA1), posterior cingulate cortex, POS1, and lateral orbitofrontal cortex (47m).

Subiculum

As shown in Figures 2 and 5, the subiculum receives strong effective connectivity from the hippocampus, presubiculum, entorhinal cortex; with some effective connectivity from posterior (31) and anterior cingulate cortex (p32, 25, a24, 10d), parietal cortex, orbitofrontal cortex (pOFC), early visual cortical areas (e.g., POS1), and prefrontal cortex (8Ad).

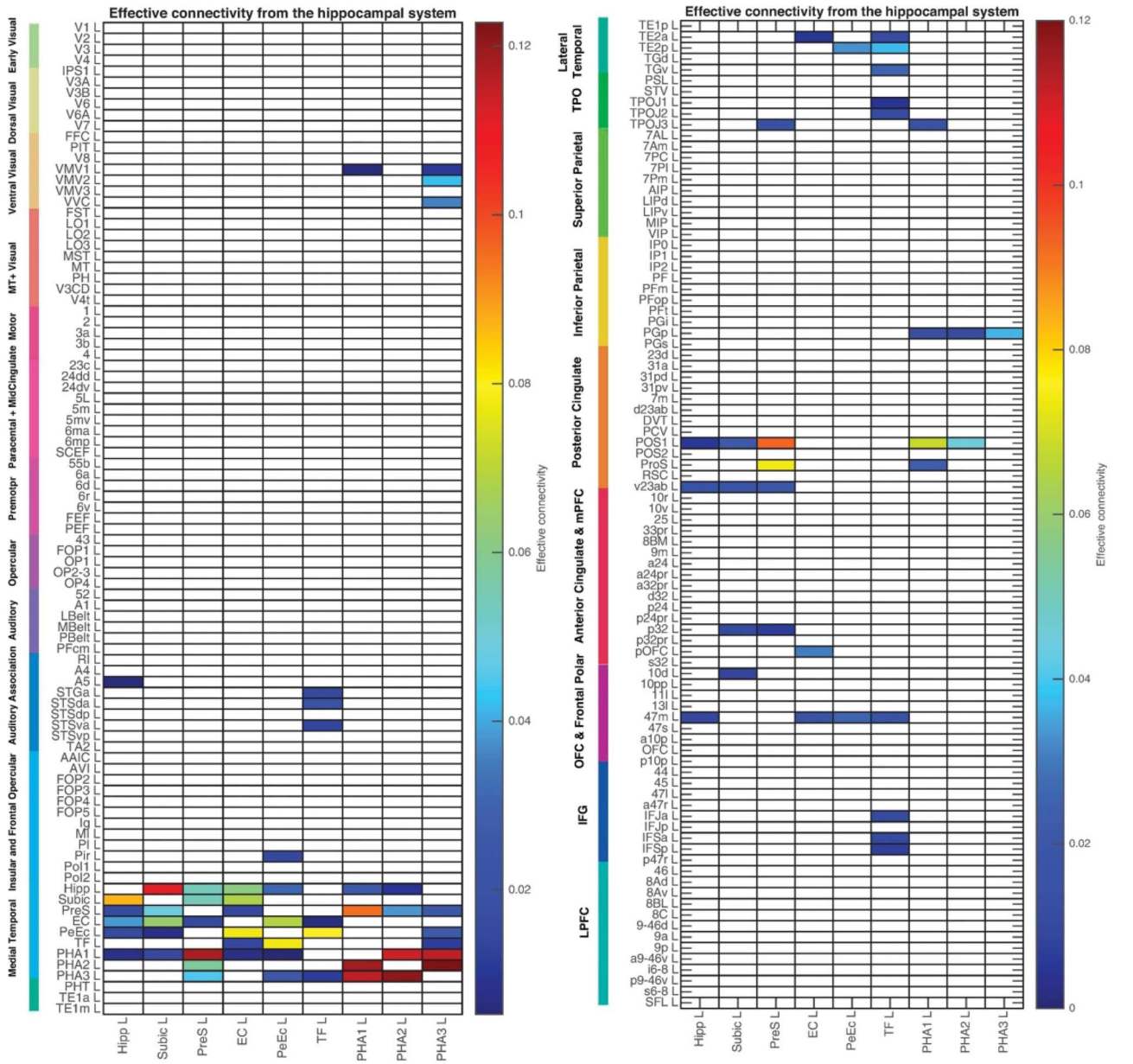

Fig. 3. Effective connectivity from the hippocampal system to all cortical areas in the left (L) hemisphere. The effective connectivity is read from a column to a row. This is calculated from 172 participants in the HCP imaged at 7T. The threshold value for the effective connectivity is 0.005. Hipp, hippocampus; Subic, subiculum; PreS, presubiculum; EC, entorhinal cortex; PeEc, perirhinal cortex; TF, parahippocampal area TF; PHA1–3, parahippocampal gyrus TH areas 1–3. The abbreviations for the other brain areas are in Supplementary Table 1, and the brain regions are shown in Supplementary Figure 1. The effective connectivity to the first set of cortical areas and the subiculum is shown on the left; and to the second set of areas on the right.

As shown in Figures 3 and 5, the subiculum has strong effective connectivity directed to the hippocampus, presubiculum, and entorhinal cortex; with some effective connectivity to parahippocampal gyrus TH, parietal cortex (PGs), posterior cingulate cortex (v23ab), early visual areas (POS1), anterior cingulate cortex (p32), orbitofrontal cortex (pOFC), anterior cingulate cortex (10d), and dorsolateral prefrontal cortex (8Ad).

Presubiculum

As shown in Figures 2 and 5, the presubiculum receives strong effective connectivity from the subiculum, parahippocampal gyrus TH, parietal cortex (7Pm, PGs), precuneus visual area (PCV) and early visual areas POS1 and ProS, and posterior cingulate cortex (31a, v23ab); with some effective connectivity from the hippocampus, entorhinal cortex, anterior cingulate cortex (p32), and dorsolateral prefrontal cortex (8Ad).

As shown in Figures 3 and 5, the presubiculum has strong effective connectivity directed to the hippocampus, subiculum, parahippocampal gyrus TH, relatively early visual areas (POS1 and ProS), and to the posterior cingulate cortex (v23ab); with weaker effective connectivity to the entorhinal cortex, anterior cingulate cortex (p32), and the dorsolateral prefrontal cortex (8Ad).

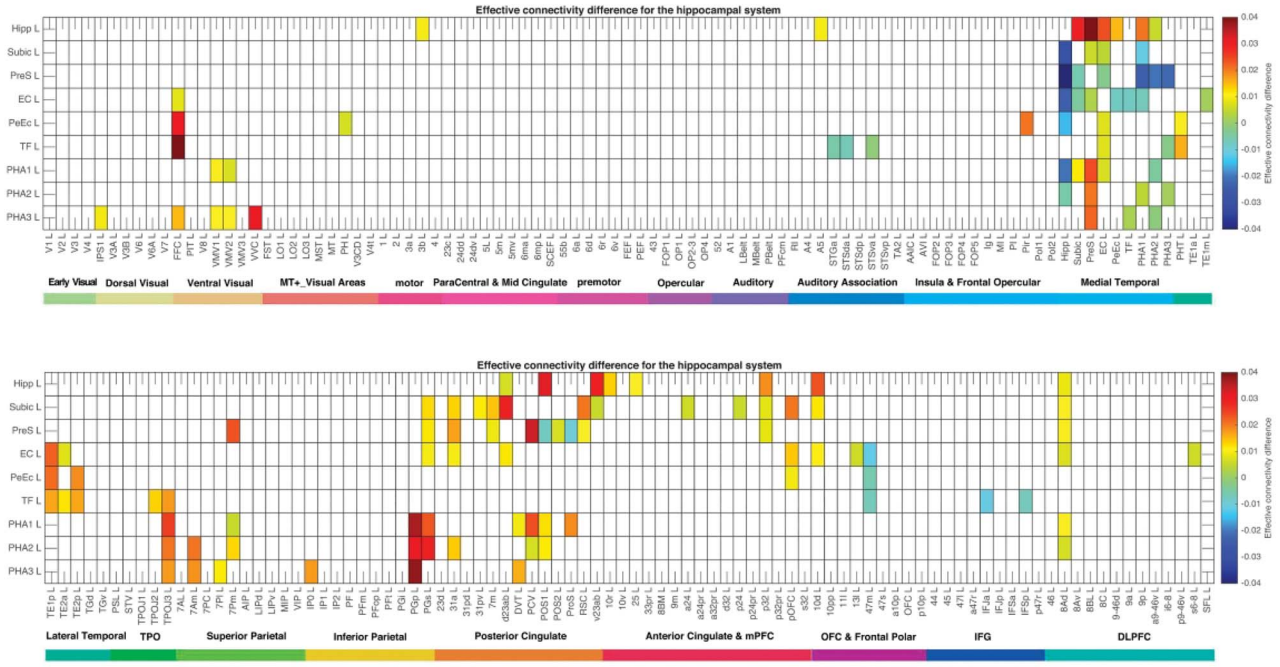

Fig. 4. Difference of the effective connectivity for the hippocampal system with cortical areas. For a given link, if the effective connectivity is positive, the connectivity is stronger in the direction column to row. For a given link, if the effective connectivity is negative, the connectivity is weaker in the direction column to row. This is calculated from 172 participants in the HCP imaged at 7T. The threshold value for any effective connectivity difference to be shown is 0.001. Hipp, hippocampus; Subic, subiculum; PreS, presubiculum; EC, entorhinal cortex; PeEc, perirhinal cortex; TF, parahippocampal area TF; PHA1–3, parahippocampal gyrus TH areas 1–3. The abbreviations for the other brain areas are shown in Supplementary Table 1, and the brain regions are shown in Supplementary Figure 1. The effective connectivity difference for the first set of cortical areas is shown above with the subiculum added; and for the second set of areas below.

Entorhinal Cortex

As shown in Figures 2 and 5, the entorhinal cortex receives strong effective connectivity from the hippocampus, subiculum, entorhinal cortex, perirhinal cortex, inferior temporal cortex (TE1p), and posterior orbitofrontal cortex (pOFC and 13l); with some effective connectivity from the presubiculum, TF, parietal cortex (PGs), posterior cingulate cortex (31a, d23ab), and anterior cingulate cortex (10d).

As shown in Figures 3 and 5, the entorhinal cortex has strong effective connectivity to the hippocampus, subiculum, and perirhinal cortex; with some effective connectivity to the presubiculum, TF, parietal cortex (PGs), anterior cingulate cortex (10d), and orbitofrontal cortex (posterior pOFC, 13l, OFC, and lateral 47m).

Perirhinal Cortex

As shown in Figures 2 and 5, the perirhinal cortex receives strong inputs from the pyriform (olfactory) cortex, the entorhinal cortex, TF, and the inferior temporal cortex (TE2p and TE1p) and fusiform face area (FFC); and weaker effective connectivity from the hippocampus, TH, posterior (pOFC) and lateral (47m) orbitofrontal cortex.

As shown in Figures 3 and 5, the perirhinal cortex has strong effective connectivity directed to the hippocampus, entorhinal cortex, and TF; and some effective connectivity to the inferior temporal cortex (TE2p)), TH, and lateral orbitofrontal cortex (47m).

Parahippocampal Cortex TF

As shown in Figures 2 and 5, the parahippocampal gyrus part TF receives strong inputs from the perirhinal cortex, and from ventral stream cortical areas (FFC, TE2a, TE2p, and TGv); and has some effective connectivity from the hippocampus, superior temporal sulcus areas (STS), and inferior frontal gyrus (IFSa).

As shown in Figures 3 and 5, the parahippocampal gyrus part TF has strong effective connectivity directed to the perirhinal cortex; with some effective connectivity to the ventral stream cortical areas (TE2a, TE2p, and TGv), STS areas, TH, the lateral orbitofrontal cortex (47m), and the inferior frontal gyrus (IFja, IFsa, IFsp).

Parahippocampal Cortex TH (Areas PHA1–3)

As shown in Figures 2 and 5, the (medial) parahippocampal gyrus part TH regions PHA1–3 are strongly interconnected, and receive strong effective connectivity from the presubiculum, the parietal cortex (e.g., PGp), and from relatively early cortical visual areas (e.g., ProS, POS1, TPOJ3) including ventromedial visual (VMV) and VVC which are part of the parahippocampal place/scene area (Sulpizio et al. 2020); and some effective connectivity from the subiculum, posterior cingulate cortex (31a), and dorsolateral prefrontal cortex (8Ad).

As shown in Figures 3 and 5, the parahippocampal gyrus part TH has strong effective connectivity directed to the hippocampus, presubiculum, the VMV areas, and

POS1; with some effective connectivity to perirhinal cortex, and the parietal cortex (e.g., PGs, PGp).

Effective Connectivity of the Nine Hippocampal System ROIs with Contralateral Cortical Areas

The contralateral effective connectivity matrices for the left hemisphere in Supplementary Figures 3 and 4 show that the nine hippocampal system regions have almost bilaterally symmetrical connectivity with the contralateral regions, though the connectivity tends to be weaker contralaterally. Apart from that the nine hippocampal system regions have much less effective connectivity with other contralateral cortical regions, apart, interestingly, from the posterior cingulate cortex. This is quite different to what can be shown as the direct connections with diffusion tractography, which connect across the midline mainly for the hippocampus, presubiculum, and TH (Huang, Rolls, Hsu, et al. 2021b). The effective connectivity analysis provides a useful and important extension in this respect to the diffusion tractography where contralateral connectivity, which tends to be long-range, is concerned. The connectivity of the nine hippocampal system regions with corresponding cortical regions contralaterally provides evidence that the effective connectivity algorithm works well, for it is contralateral corresponding cortical regions that have the strongest effective connectivity.

Effective Connectivity of the Nine Hippocampal System Regions with Subcortical Areas

The hippocampus had effective connectivity with the amygdala (To = 0.065, From = 0.052, contralaterally a little lower at 0.061 and 0.046) and septum (To = 0.011, From = 0.031, contralaterally only From = 0.016). The subiculum had effective connectivity from the forebrain nucleus basalis of Meynert (0.021) and some from the septum (0.015). The entorhinal cortex had effective connectivity to the amygdala (0.019). The perirhinal cortex had effective connectivity with the amygdala (To = 0.051, From = 0.031), and weakly from the nucleus basalis (0.007). The septum and basal nucleus, mapped in humans, contain cholinergic neurons (Mesulam 1990; Zaborszky et al. 2008; Zaborszky et al. 2018). TF had effective connectivity to the amygdala (0.015), and PHA1–3 did not correctly in our typescript.

Difference of the Effective Connectivities in the Two Directions in the Hippocampo-Cortical System

To help reveal what the effective connectivity can show that is different from FC or anatomical connections, Figure 4 shows the difference of the effective connectivity in the two directions for each link in the hippocampo-cortical system. For a given link, if the effective connectivity shown in Figure 4 is positive, the connectivity is stronger in the direction from column to row. Conversely, for a given link, if the effective connectivity shown in Figure 4 is negative, the connectivity is weaker in the direction from column to row. The interpretation of Figure 4 is as follows. The effective connectivity is stronger in the direction from column to row for most of the effective connectivity links. For example, parietal cortex area PGp has stronger effective connectivity to parahippocampal TH (PHA 1–3) than in the reverse direction. Most of these positive effective connectivity links are as expected, given understanding of cortico-hippocampal function, for these cortical areas are driving strong forward inputs into the hippocampal system, with weaker connectivity in the back projection direction from the hippocampal system for memory recall (Rolls 2016, 2021d), as considered in the Discussion. One great exception in Figure 5 to the directionality of the links is that the effective connectivity is weaker from the hippocampus to the other hippocampal system areas such as the subiculum, presubiculum, entorhinal cortex, than in the other direction. This is very consistent that these hippocampal connectivities are back projections used for memory recall, for they must be weak in this back projection direction for memory systems to operate correctly, as considered in the Discussion.

Validation of the Effective Connectivity Algorithm

As this is the first use of this asymmetric Hopf effective connectivity algorithm that measures connectivity in both directions, steps were taken in a number of ways to validate it.

First, its performance was evaluated in a brain system in which the connectivity is relatively well understood using anatomy in nonhuman primates. In particular, it is expected that there is a hierarchy from V1 to V2 to V4, with the connections stronger in the forward direction than in the reverse direction, due to the asymmetric connections in the forward and backward directions between each pair of cortical areas (Markov et al. 2013; Markov and Kennedy 2013; Markov, Ercsey-Ravasz, et al. 2014a; Markov, Vezoli, et al. 2014b; Rolls 2016). The effective connectivity between these areas measured with the present algorithm is consistent with this anatomy, as set out in the Supplementary Material including Supplementary Figure 5.

Second, it was important to assess whether the operation of the Hopf effective connectivity algorithm could operate independently of any evidence from the anatomical structural connectivity. The algorithm can utilize evidence from the anatomy about which connections are not present in the brain, because reducing the number of connectivities that have to be computed by the algorithm may help it to converge faster or more accurately (Deco et al. 2019). But if the effective connectivity algorithm is to provide support, it would be helpful to know whether it can calculate the same effective connectivity without any structural anatomical information. This was tested by replacing the structural connectivity matrix used by the algorithm with a matrix of zeros. It was found that the effective connectivity matrix computed using the structural anatomical versus zero matrices was correlated with r=0.97. Thus the effective connectivity

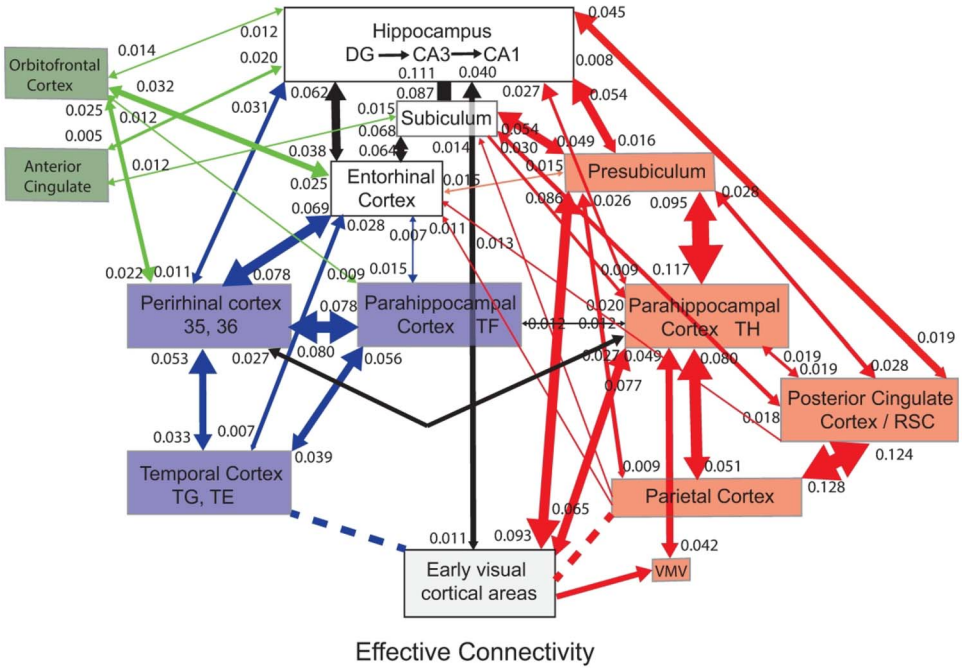

Fig. 5. Summary of the effective connectivity of the human hippocampal system measured across all 172 HCP participants at 7T. The maximum value of the effective connectivity is 0.2, and the strength in each direction is shown close to the termination of an arrow. The width of the arrows and the size of the arrowheads reflect the strength of the effective connectivity. For areas such as the temporal lobes, the parietal cortex, and the posterior cingulate cortex, there are several subregions in the HCP atlas, and the value of the strongest effective connectivity to or from any subarea is shown in this case. Brain regions that are part of the ventral "what" stream are shown in blue color, that are part of the dorsal "where" or "action" stream are shown in red color, and that involve the orbitofrontal and anterior cingulate cortex reward value stream are in green color. The VMV areas and TH include the parahippocampal place/scene area. The early visual areas referred to here include POS1 and ProS. Effective connectivities of less than 0.010 in the stronger direction are not included for clarity, but are shown in Figures 2 and 3. Dashed lines indicate that there are several stages to the connectivity. The summary figure focuses on connectivity of hippocampal system brain regions and does not show connectivity between other brain systems such as the orbitofrontal cortex and lateral temporal cortex TE and TG.

algorithm described here can compute effective connectivity that is independent of any input from the structural connectivity, and that procedure starting with zeros was used here. This enables these two types of independent evidence, from diffusion tractography (for the hippocampal system, see, e.g., Huang, Rolls, Hsu, et al. 2021b) and from effective connectivity, to be brought to bear on the connectivity of the human brain.

Third, the great consistency in the direction of the effective connectivity shown in Figure 4 across many connectivity links, and the way in which these connectivities fit with understanding of the operation of cortical memory systems (Rolls 2016, 2021d), provides evidence on the robustness and utility of the algorithm described here, even when measuring effective connectivity between 428 brain regions.

Summary of the Effective Connectivity of the Human Hippocampal System

Figure 5 shows a summary of the effective connectivity of the hippocampal system measured here across all 172 participants. The maximum value of the effective connectivity is 0.2, and is shown for each link where the connectivity in either direction is ≥0.010 in Figure 5. The width of the arrows and the size of the arrow heads reflect the strength of the effective connectivity. For areas such as the temporal lobes, the parietal cortex, and the posterior cingulate cortex, there are several regions in the HCP atlas, and the value of the strongest effective connectivity to or from any region is shown in this case.

First, it is clear that the visual "what" system (blue in Fig. 5) projects from the temporal lobes with generally stronger forward effective connectivity toward the hippocampus via the perirhinal cortex and entorhinal cortex. However, there is generally effective connectivity also in the backward direction, away from the hippocampus, and this may be useful in memory recall (Treves and Rolls 1994; Rolls 2021d).

Second, it is interesting in humans that the lateral part of the parahippocampal gyrus, TF, is strongly connected with and is part of this ventral stream, in terms of its effective connectivity. (In macaques, the understanding was that the parahippocampal gyrus is interposed between parietal/posterior cingulate areas and the hippocampus [Van Hoesen 1982].)

Third, the ventral stream connectivity is not purely hierarchical, but instead the effective connectivity operates in part to jump across layers of the hierarchy. For example, the hippocampus has bidirectional effective connectivity with the perirhinal cortex, in addition to the effective connectivity involving the entorhinal cortex; the entorhinal cortex has effective connectivity between it and temporal cortical visual areas, in addition to the connectivity via the perirhinal cortex.

Fourth, in the visual "where" or "action" system (red in Fig. 5), the system is not strictly hierarchical. There is

connectivity from parietal cortex via posterior cingulate cortex directly to the hippocampus; and via posterior cingulate cortex via parahippocampal TH and presubiculum to and from the hippocampus. In addition, there is a pathway from early visual cortical areas via the VMV area which together with the parahippocampal TH include the parahippocampal place area (Sulpizio et al. 2020) that projects via the presubiculum to the hippocampus. Furthermore, the presubiculum has some effective connectivity with early visual cortical areas (including POS1 and ProS); and also via TH and the posterior cingulate cortex then parietal cortex with early visual cortical areas (see above and Figs 2 and 3).

Fifth, a point of interest in this system is that in terms of effective connectivity (and anatomically; Huang, Rolls, Hsu, et al. 2021b), the presubiculum appears in the dorsal visual system to be topologically equivalent to the entorhinal cortex for the (mainly) ventral visual system. In humans, the presubiculum is largely posterior to the entorhinal cortex (Figs 1 and Supplementary Fig. 1; Huang, Rolls, Feng, et al. 2021a), and so is in a good position to provide for connections between the hippocampus and parietal, posterior cingulate, and early visual areas that are relatively posterior.

Sixth, the effective connectivity indicates that in humans it is the TH part of the parahippocampal gyrus that is part of the dorsal visual route to and from the hippocampus.

Seventh, the posterior cingulate cortex has interesting effective connectivity with the hippocampal system, for it has strong forward connectivity to the hippocampus, with relatively weak backward effective connectivity.

Eighth, the subiculum has strong effective connectivity with both the entorhinal cortex and presubiculum, and also with the hippocampus, and provides a route that is additional to the direct connectivity of the entorhinal cortex and presubiculum with the hippocampus. The subiculum is thus a potentially interesting area in terms of convergence of the ventral and dorsal stream connectivity with the hippocampus.

Ninth, the orbitofrontal and anterior cingulate cortex, implicated in reward and emotion processing (Rolls 2019a, 2021a; Rolls, Cheng, Feng 2020a), has interestingly moderate effective connectivity with the hippocampus, subiculum, entorhinal cortex, and perirhinal cortex. This provides evidence for connectivity for reward information to reach the hippocampal system (e.g., to become part of an episodic memory), and to return from the hippocampus (e.g., during the retrieval of an episodic memory) (Rolls 2021a). The orbitofrontal cortex, ventromedial prefrontal cortex, and anterior cingulate cortex thus in terms of effective connectivity constitute a third stream of effective connectivity to and from the hippocampus, as shown, in green color, in Figure 5. It is notable that the hippocampal connectivity of this third stream is more with the orbitofrontal cortex and the ventromedial prefrontal cortex than with the anterior cingulate cortex (Fig. 5, see also Figs 2 and 3).

Tenth, the connections of the hippocampal system with the prefrontal cortex system for short-term memory appear to be interestingly organized (Fig. 3). The parahippocampal TH area implicated in place/scene spatial representations (and the hippocampus, subiculum, and presubiculum) is interconnected with the dorsolateral prefrontal cortex area 8Ad, which is probably part of the frontal eye field used to remember where the eyes have been fixating in space (Funahashi et al. 1989) and is involved in top-down attention (Germann and Petrides 2020) that requires short-term memory to hold the object of attention online (Deco and Rolls 2005; Rolls 2021d). In contrast, the perirhinal cortex is connected with the lateral prefrontal cortex (p9–46), and TF is especially interconnected with the inferior frontal prefrontal cortex areas, which is of interest for this interconnectivity may be involved more in "what" short-term memory (Rolls 2021d). Also, area 10, the frontal pole, implicated in planning (Gilbert and Burgess 2008; Shallice and Cipolotti 2018), has effective connectivity with the hippocampus, presubiculum, and entorhinal cortex (Fig. 3).

Eleventh, it is evident that some early sensory cortical areas have connectivity with the hippocampal system. For vision, one such key early visual area is POS1, which is located just adjacent to V1 (see brain diagrams; Huang, Rolls, Feng, et al. 2021a; Huang, Rolls, Hsu, et al. 2021b). The details of this connectivity revealed by the analysis performed here are that V1 and V2 have effective connectivity to ProS = 0.078; ProS then has effective connectivity to POS1 = 0.043; and POS1 then has effective connectivity to the Hipp = 0.038. There is thus a pathway from early visual cortical areas to the hippocampus. That is reflected in the diffusion tractography (Huang, Rolls, Hsu, et al. 2021b), and the effective connectivity further extends the diffusion tractography by showing that the strong connections between the same early visual cortical areas and the presubiculum and TH (PHA1) are reflected in high effective connectivity from these early visual cortical areas directed toward these hippocampal system areas. Similarly, there was effective connectivity from other sensory systems to the hippocampal system, including pyriform (olfactory) cortex, somatosensory cortex, and auditory area A5 (Fig. 2).

Some of the implications of the effective connectivity shown in Figure 5 are considered in the Discussion.

Discussion

Effective Connectivity and Connections of the Human Hippocampal System

The effective connectivity of the human hippocampal system described here and summarized in Figure 5 is very helpful to compare with the direct anatomical connections of the hippocampal system as revealed by diffusion tractography in the same individuals (Huang, Rolls, Hsu, et al. 2021b) and shown here in

Supplementary Figure 2 for comparison. The effective connectivity supports new key findings about the anatomical direct connections in humans (Huang, Rolls, Hsu, et al. 2021b), by showing functional correlates that are measured independently of any anatomical information, and using only BOLD signals recorded with fMRI. We focus on these comparisons in this section, and consider their implications later. The effective connectivity measurements in addition go beyond the diffusion tractography, by providing evidence on the direction of the connectivity, and on its physiological strength measured by effects on signals as compared with streamline numbers.

First, the human hippocampus has more extensive anatomical direct connections with cortical areas as shown by diffusion tractography than in even nonhuman primates, including with some parietal cortex areas, the posterior and retrosplenial cingulate cortex, the temporal pole, and even with early sensory areas for vision, olfaction, and somatosensation (Huang, Rolls, Hsu, et al. 2021b) (see Supplementary Fig. 2 that summarizes the anatomical connections measured with diffusion tractography). The effective connectivity described here extends that evidence, by confirming that there is effective connectivity between the hippocampus and most of these cortical areas (Figs 2–5). The effective connectivity also shows that the connectivity with early sensory areas is stronger toward the hippocampal system, so may provide for some low-level sensory details to be stored with each episodic memory, which could help to make human episodic memory vivid because some lower level sensory detail can be incorporated that may not be represented in areas higher in the hierarchy including, for example, the perirhinal cortex. The effective connectivity was measured in the resting state, and it is possible that during an imagery task, the connectivity from the hippocampus to early sensory areas might be stronger. Based on research in macaques, some of the connections to the hippocampus are direct to hippocampal CA1, rather than through the trisynaptic circuit from the dentate gyrus and CA3 to CA1. For example, direct projections to CA1 in macaques have been reported from areas 7a and 7b, area TF, and a region in the occipitotemporal sulcus (Rockland and Van Hoesen 1999; Ding et al. 2000), and from superior temporal sulcus, the rostral and retrosplenial portions of the cingulate cortex, the agranular insular cortex, and the caudal orbitofrontal cortex (Suzuki and Amaral 1990); and also from anteroventral TE (Zhong and Rockland 2004). That raises the important concept that in humans (and to some extent in nonhuman primates) direct inputs to CA1 may be combined with the output of CA3 to enable detailed cortical information to be combined in CA1 with what is recalled via the CA3 input to CA1.

Second, a key finding of the tractography related to the above is that the human hippocampus has direct connections with the perirhinal cortex and parahippocampal gyrus areas TF and TH (Huang, Rolls, Hsu, et al. 2021b). That suggested that the entorhinal cortex is not the primary and exclusive gateway to and from the hippocampus in humans. The effective connectivity of the entorhinal cortex described here supports this concept for humans, in that the entorhinal cortex has effective connectivity with fewer cortical areas than the hippocampus (Figs 2–5). The concept that the entorhinal cortex is not the primary and exclusive gateway to and from the hippocampus in humans is supported by evidence from macaques (Rosene and Van Hoesen 1977; Barbas and Blatt 1995; Blatt and Rosene 1998; Insausti and Munoz 2001).

A third key observation was that the effective connectivity of the human presubiculum makes it appear as an equivalent for the dorsal visual cortical stream to the entorhinal cortex for the ventral stream, as set out in Figure 5, and in fact the tractography fits this too, as shown in Supplementary Figure 2. In particular, the presubiculum receives inputs from the parietal cortex, the parahippocampal gyrus TH, and the posterior cingulate cortex, and has strong bidirectional connections with the hippocampus (Fig. 5). However, this is not to say that the entorhinal cortex does not provide a route for dorsal stream inputs to reach the hippocampal trisynaptic circuit, for the entorhinal cortex does have effective connectivity directed toward it from the presubiculum and posterior cingulate/retrosplenial cortex (Figs 2–4). Consistent with what was found here for humans (Figs 2–5), in the monkey the presubiculum receives a strong input from area 7 of the posterior parietal cortex (Seltzer and Van Hoesen 1979) and the posterior cingulate cortex (Bubb et al. 2017), and the monkey presubiculum projects to the posterior part of the entorhinal cortex (Witter and Amaral 2021). The macaque presubiculum contains head direction cells (Robertson et al. 1999).

The subiculum has strong bidirectional effective connectivity with the hippocampus, entorhinal cortex, and presubiculum, and thus has connectivity with both the dorsal and ventral processing streams. Although anatomically the hippocampus classically projects to the subiculum and the presubiculum, the effective connectivity from the subiculum and the presubiculum to the hippocampus, evident in Figures 3 and 5, could arise via direct connections to CA1 from the subiculum (demonstrated in rodents and rabbits) (Xu et al. 2016), via connections involving nearby cortical areas such as the entorhinal cortex, or via subcortical areas including the thalamus (Bubb et al. 2017). The subiculum and the hippocampus represent information about linear and angular whole body motion, and the signals that can drive these neurons can be vestibular or optic flow, or both (O'Mara et al. 1994). (What are probably similar cells have been described in the rodent medial entorhinal cortex, but have been termed "speed cells" [Kropff et al. 2015].) The subiculum has effective connectivity with parietal PG areas, and with the posterior cingulate cortex, which are likely to be part of the same system. Consistent

with this, vestibular and optic flow signals are found in the parietal cortex of primates in area 7a (Wurtz and Duffy 1992; Bremmer et al. 2000; Avila et al. 2019; Cullen 2019), and activations in humans to optic flow are found in early visual cortical areas such as 6A (Sherrill et al. 2015), which may be sources of input to the hippocampus and the subiculum that drive the whole body motion neurons (O'Mara et al. 1994).

A fourth key finding of the tractography is that the parahippocampal gyrus is not mainly for connections with the dorsal visual system/parietal areas, as in the dual stream model (see Van Hoesen 1982; Suzuki and Amaral 1994; Burwell et al. 1995; Burwell 2000; Knierim et al. 2014; Doan et al. 2019). Instead, the effective connectivity also strongly supports the diffusion tractography (Huang, Rolls, Hsu, et al. 2021b) in that in humans, area TF, which is lateral and extends relatively anterior, is connected with ventral stream "what" areas (Figs 2–5) (and this is supported by connections of TF to the perirhinal cortex in macaques; Suzuki and Amaral 1994). It was also interesting that TF had connectivity with the inferior frontal gyrus areas involved in short-term memory (Rolls 2021d). In a complementary way, area TH of the parahippocampal gyrus (proisocortical, and possibly of early evolutionary origin; Pandya et al. 2015), which is more medial and extends more posterior, appears to provide the effective connectivity between the hippocampus and dorsal stream areas including parietal and posterior cingulate areas including the retrosplenial cingulate cortex. This supports the human tractography (Huang, Rolls, Hsu, et al. 2021b). Moreover, the effective connectivity reveals that it is especially area TH (compared to TF), that with the presubiculum, has strong effective connectivity with early sensory areas. Area TH (PHA1–3) and the adjacent posterior VMV regions include the parahippocampal place area that responds to spatial scenes (Sulpizio et al. 2020), and it is via this route that hippocampal and parahippocampal spatial view cells (Rolls et al. 1997, 1998, 2005; Robertson et al. 1998; Georges-François et al. 1999; Rolls and Xiang 2005, 2006; Wirth et al. 2017; Rolls and Wirth 2018; Tsitsiklis et al. 2020; Rolls, 2021d, 2021e) are likely to receive inputs.

A fifth key finding from the effective connectivity is that this extends bilaterally (Supplementary Figs 3 and 4). This is an important extension of the diffusion tractography, which does not generally reveal interhemispheric connections as well as it does intrahemispheric connections (Huang, Rolls, Hsu, et al. 2021b). The pattern of connections to contralateral areas of the hippocampal system is interesting, for although the contralateral effective connectivity is weaker than the ipsilateral, the areas with which there is connectivity correspond well, as shown in Figures 2 and 3. It is noted that if there are only relatively minor connections between the CA3 regions in the two hemispheres of the human hippocampus this would enable the human CA3 attractor network of the hippocampus to operate as two separate attractor networks, allowing the left human hippocampus to specialize more for language-related functions (Rolls 2018a, 2021d). This would effectively double the memory capacity of the human hippocampus, as the capacity is determined largely by the number of CA3–CA3 connections per neuron in each separate attractor network (Rolls 2018a, 2021d). Consistent with this, in macaques there are relatively few CA3–CA3 interhemispheric connections (Amaral et al. 1984).

A sixth finding was evidence for effective connectivity between areas in the ventral and dorsal streams before the level of the entorhinal cortex and presubiculum (Fig. 5). As expected, both ventral stream and dorsal stream areas had effective connectivity with the entorhinal cortex (Fig. 5). But before this level, there was bidirectional effective connectivity between the perirhinal cortex and TH (0.025) (Figs 2–5); and between TF and TH (0.003). This provides support for the tractography which provided evidence for connections between the dorsal and ventral streams (Huang, Rolls, Hsu, et al. 2021b; Supplementary Fig. 2). This provides evidence for incomplete segregation of "what" and "where" streams, thus going beyond the simple dual stream model illustrated in Figure 1 of Huang, Rolls, Hsu, et al. (2021b) (Supplementary Fig. 2).

Seventh, Figures 2 and 3 make it evident that an area with which the human hippocampal system does have effective connectivity, via parahippocampal gyrus TF, is with the human anterior temporal lobe (TG). This supports the diffusion tractography (Huang, Rolls, Hsu, et al. 2021b, Fig. 5), which indicates connections in humans between TG and perirhinal, TF and the hippocampus, with weaker connections of TG with the entorhinal cortex. This may be important in relation to language, as the human left anterior temporal lobe is implicated in semantic representations (Bonner and Price 2013; Pascual et al. 2015; Rolls 2021d). Indeed, it must be remembered that the formation of new semantic representations, as well as episodic memory, is impaired by hippocampal damage (Rolls 2021a), and the connectivity especially with the anterior temporal lobe provides clues about this functionality. Indeed, TF is a very interesting area in humans, for it has effective connectivity not only with the perirhinal cortex and thereby with the hippocampus, but also with the cortex in the superior temporal gyrus that has auditory functions, with TE areas with high-level visual functions and the fusiform face area, with the inferior frontal gyrus involved in short-term memory and that are very close to Broca's area (BA 45), and with the orbitofrontal cortex (Fig. 3) (Rolls 2021d). This connectivity suggests that TF in humans may have a role in language and semantic processing, and consistent with this, concrete nouns that can be perceived visually activate the left parahippocampal gyrus (Mayer et al. 2017).

Eighth, there is effective connectivity of the hippocampus with many auditory cortex areas (Figs 2 and 3), but this is likely to be mediated through direct connections of the hippocampus with region STGa with which the

hippocampus does have direct connections (Fig. 5 of Huang, Rolls, Hsu, et al. 2021b). (This is supported by evidence in macaques, in which the entorhinal, perirhinal, and parahippocampal cortices have connections with auditory association areas in the superior temporal sulcus [Insausti et al. 1987; Suzuki and Amaral 1994; Lavenex et al. 2002; Munoz and Insausti 2005].)

Ninth, the moderate effective connectivity of the hippocampus with prefrontal cortex areas 10 and 8 (Figs 2 and 3) is likely to be trans-synaptic, as it is not evident in the tractography (Fig. 5 of Huang, Rolls, Hsu, et al. 2021b).

Tenth, it is of interest that most parts of the hippocampal system described here have effective connectivity with prefrontal area 8, especially 8Ad at the junction of the superior and middle frontal gyri (Figs 2 and 3). This was not evident in the tractography, so this is probably a trans-synaptic connection. This is probably part of the frontal eye fields that have extensive connectivity with dorsal visual stream areas (Passingham 2021), and which are involved in eye movements to remembered targets (Funahashi et al. 1989; Goldman-Rakic 1996). The hippocampal spatial view representation of scenes by spatial view cells (Rolls and Xiang 2006; Rolls and Wirth 2018; Rolls 2021d, 2021e) that can be updated by eye position self-motion (Robertson et al. 1998; Wirth et al. 2017) may relate to this brain area when the movements have to be remembered, as they do for idiothetic update (Rolls 2020, 2021e). Area 8A is also implicated in visual and auditory top-down attention (Germann and Petrides 2020), which requires a short-term memory to hold online the target for attention (Deco and Rolls 2005; Ge et al. 2012; Rolls 2021d).

Comparisons with Macaque Neuroanatomy

Many of the findings described here go beyond what is known in rodents, because of the great development of many cortical systems in humans including in the orbitofrontal, cingulate, and visual cortical areas, but receive support from neuroanatomical tract-tracing studies in macaques as described next. Some homologies between the macaque and human hippocampal formation have been described (Insausti and Amaral 2004). The effective connectivity in humans of course goes beyond what is known in macaques, partly because many of these cortical systems are more developed in humans, partly because effective connectivity measures the strength of physiological effects, and partly because effective connectivity may reveal some trans-synaptic effects.

The effective connectivity of the human entorhinal cortex described here includes connectivity with parahippocampal TF and TH, with perirhinal cortex, with some posterior cingulate and anterior cingulate regions, with the medial (13) and lateral (47) orbitofrontal cortex, and with prefrontal area 8A, and anatomical afferents to entorhinal cortex from generally similar regions are found in macaques (Insausti et al. 1987). The effective connectivity of the entorhinal cortex with inferior temporal TE and inferior parietal PG described here is probably trans-synaptic (via perirhinal and parahippocampal cortex, or even via the hippocampus; Huang, Rolls, Hsu, et al. 2021b), because it is not evident in the human diffusion tractography (Huang, Rolls, Hsu, et al. 2021b), and is of limited extent in macaque neuroanatomy (Insausti et al. 1987; Saleem and Tanaka 1996). In macaques, the entorhinal cortex receives from the cortex in the superior temporal sulcus (Insausti et al. 1987), but that was not evident in the human STS auditory regions in the effective connectivity or diffusion tractography (Huang, Rolls, Hsu, et al. 2021b), but this could be related to the development of the middle temporal gyrus in humans which may contain some of the macaque's STS regions that represent face expression and vocalization (Hasselmo et al. 1989; Cheng et al. 2015). The entorhinal cortex in humans also has connectivity with three somatosensory areas (Fig. 2). In macaques, analogous connections with sensory areas are less evident (Insausti et al. 1987) than in rodents (Insausti et al. 1997; Burwell and Amaral 1998).

The hippocampus has effective connectivity in humans with expected areas such as the entorhinal cortex, subiculum, and presubiculum, but in addition has effective connectivity with the perirhinal cortex, inferior parietal (PG), anterior cingulate, posterior cingulate, and orbitofrontal cortex, supporting most of the diffusion tractography (Huang, Rolls, Hsu, et al. 2021b), and also supported by macaque neuroanatomy (Suzuki and Amaral 1990; Barbas and Blatt 1995; Rockland and Van Hoesen 1999; Ding et al. 2000; Insausti and Munoz 2001), though connections from the hippocampus to the posterior cingulate cortex may not have been reported in macaques.

The connectivity of TF, shown in Figures 2 and 3, with early visual cortical areas is supported by the diffusion tractography in the same participants (Huang, Rolls, Hsu, et al. 2021b), and by connections in macaques of V2, V3, and V4 to parahippocampal gyrus TF (Felleman and Van Essen 1991; Lavenex and Amaral 2000; Lavenex et al. 2002).

In humans, the effective connectivity of the hippocampal system to contralateral areas is less strong and less extensive than ipsilaterally (compare Supplementary Figs 3 and 4 with Figs 2 and 3), and this is supported by evidence from macaques (Amaral and Cowan 1980; Insausti et al. 1987).

Implications for Understanding Hippocampal Function as a System Involved in Memory and Navigation in Humans

The wider implications of the effective connectivity and connections described above are now considered.

First, the hippocampus receives effective connectivity (in some cases via regions such as the perirhinal cortex) from a number of sensory processing areas early in the cortical hierarchies including somatosensory cortex (3b), auditory cortex (A5), piriform (olfactory) cortex, and

early visual cortex (POS1, POS2, and ProS) (Figs 2–5 and Supplementary Fig. 5). It is suggested that this enables some low-level sensory information to be included in human episodic memory. There are, in most cases, return pathways, generally weaker, that provide for this type of information to be recalled to early sensory cortical areas during the recall of episodic memories (Treves and Rolls 1994; Rolls 2016). In the case of vision, the effective connectivity is especially strong with POS1, which is close to V1 and V2 (see Supplementary Fig. 1 and Huang, Rolls, Feng, et al. (2021a)), with the effective connectivity path V1 and V2 to ProS (EC = 0.08), which in turn connects with POS1 (EC = 0.05) (Supplementary Fig. 5).

Second, the hippocampus and entorhinal cortex have effective connectivity with the orbitofrontal cortex (including the medial pOFC and the lateral 47 m) and the anterior cingulate cortex (p32 and 25), which represent reward and punishment value, and are involved in emotion (Rolls 2014, 2018b, 2019b, 2019a; Rolls, Cheng, Feng 2020a). Part of the importance of this is that remembering where rewards have been seen in the world is an important part of episodic memory, which is reflected in neurons that respond in macaques to rapidly learned locations of rewards in viewed spatial scenes (Rolls and Xiang 2005). Even more, by providing the value component to episodic memory, this orbitofrontal/anterior cingulate relationship of the human hippocampus may lead to greater processing of episodic memory if the recalled episodic memory has some value component, and thus to whether that information is consolidated into semantic neocortical memory (Rolls 2021a). This provides a new approach (Rolls 2021a) to understanding the role of the ventromedial prefrontal cortex/anterior cingulate cortex in memory (Bonnici and Maguire 2018; McCormick et al. 2018; McCormick et al. 2020). The orbitofrontal/ventromedial prefrontal cortex connectivity to and from the hippocampus can be considered as a third stream of processing for the hippocampal system in addition to the ventral "what" and dorsal "where" streams (Fig. 5). These three processing streams thus together provide the information to the hippocampus that enable three key components of episodic memory, "what," "where," and "reward/emotional value," to be associated together in the CA3 attractor network, for later recall from any of the three components (Rolls 2021a).

Third, the effective connectivity of the human hippocampal system described here is consistent with the hypothesis that it is not organized as a strictly hierarchical system from neocortex via perirhinal cortex/parahippocampal gyrus via entorhinal cortex to and from the hippocampus (Fig. 5). A consequence is that each stage does not need to be relied on as a primary route to and from the hippocampus, and this in turn may allow different areas to specialize in different functions. For example, the parahippocampal gyrus TH (PHA1–3) receives from the VMV areas, and together they include the parahippocampal place (or, in fact, scene) area (Sulpizio et al. 2020). This is likely to be a route for hippocampal spatial view cells to receive their inputs about locations in spatial scenes (Rolls et al. 1997; Georges-François et al. 1999; Tsitsiklis et al. 2020), which are important not only for memory (Rolls et al. 2005; Rolls and Xiang 2005; Rolls and Xiang 2006; Kesner and Rolls 2015), but also for navigation (Rolls and Wirth 2018) from landmark to landmark (Rolls 2021e). Spatial view cells can be updated by self-motion in the dark (Robertson et al. 1998), which may be valuable in navigation if a part of the scene is temporarily obscured (Rolls 2021e), and these inputs for idiothetic update may reach the hippocampus from the dorsal visual stream via the parietal cortex which is implicated in this computation (Rolls 2020), and which projects to the human hippocampus (Figs 2 and 5). These multiple routes to and from the hippocampus may also allow specialization of parts of the entorhinal cortex, with the medial entorhinal cortex implicated in grid cells for place (Moser et al. 2015) and view (Meister and Buffalo 2018; Garcia and Buffalo 2020), and the lateral entorhinal cortex implicated in generating time within the hippocampal system (Tsao et al. 2018; Rolls and Mills 2019). Another possible specialization is parahippocampal cortex TF (which is lateral), which is not only linked with the human ventral visual system, but which also has effective connectivity that is prominent with the anterior temporal lobe (TG) implicated in semantic memory (Bonner and Price 2013), with A5 and the superior temporal gyrus/sulcus areas implicated in auditory and semantic processing including word-form recognition (DeWitt and Rauschecker 2013; Rolls 2021d), and with the inferior frontal gyrus (IFsa, IFja, IFSp) that is implicated in short-term memory and has strong connectivity with Broca's areas 44 and 45 (for TF on the left but not on the right) (EC = 0.07) (Rolls 2021d). This links left TF to, at least, short-term memory and perhaps to language. Another interesting region suggested for further study in relation to understanding human hippocampal function better is POS1, because of its strong effective connectivity with the hippocampal formation (Figs 2, 3, and Supplementary Fig. 5).

Fourth, not only does the hippocampus have strong effective connectivity directed to the subiculum and presubiculum, consistent with traditional concepts, but also both have strong connectivity directed to the hippocampus (Figs 3 and 5). There is some anatomical support for this in that there is now evidence from nonhumans for connections from the subiculum to CA1 (Xu et al. 2016). This deserves further exploration.

Fifth, although the ventral and dorsal visual routes to and from the hippocampus are moderately separate (Fig. 5), providing an important role for the hippocampus to associate together "what" and "where" representations for episodic memory (Kesner and Rolls 2015; Rolls 2018a), there are moderate (EC = 0.027) interactions between the perirhinal cortex and medial parahippocampus gyrus TH (Fig. 5), raising the possibility for

some representations to be built in these regions that reflect a combination of information from the ventral and dorsal visual streams. These cross-connectivities between the processing streams are supported by the diffusion tractography in humans (Huang, Rolls, Hsu, et al. 2021b) and by findings in macaques (Felleman and Van Essen 1991; Suzuki and Amaral 1994; Buffalo et al. 2006) and rodents (Burwell et al. 1995; Furtak et al. 2007; Ranganath and Ritchey 2012; Knierim 2015).

Sixth, the effective connectivity analyses described here go beyond diffusion tractography and FC by providing evidence on the directionality of the connectivity. This is brought out by the analysis shown in Figure 4. For most of the links shown in Figure 4, the effective connectivity is stronger in the direction from cortical areas to the hippocampal system, indicated by a positive difference of connectivity for a link in Figure 4. For example, parietal cortex area PGp has stronger effective connectivity to parahippocampal TH (PHA1–3) than in the reverse direction. The interpretation is that these cortical areas are driving strong forward inputs into the hippocampal system, with weaker connectivity in the back projection direction from the hippocampal system for memory recall (Rolls 2016, 2021d). The concept is that, for example, the entorhinal cortex must strongly drive the hippocampus to help force memories into storage in the hippocampus, and then the hippocampal back projection can be weak so that it recalls, and does not dominate activity in the entorhinal cortex (Treves and Rolls 1994; Rolls 2016, 2021d). Part of the importance of weaker back projections than forward projections in memory systems is that perception should always be dominated by forward, bottom-up, inputs from the world, otherwise the individual could become locked into a world dominated by memories, rather than responding to the environment, as described elsewhere with computational analyses (Rolls 2016, 2021d). Indeed, the ratio of forward to back projection strength is lower in schizophrenia, and it is proposed that this may contribute to domination by internal thoughts and disconnection from the real world in schizophrenia (Rolls, Cheng, Gilson, et al. 2020b). One great exception in Figure 4 to the directionality of the links is that hippocampal connectivity is weaker from the hippocampus to the other hippocampal system areas subiculum, presubiculum, and entorhinal cortex, than in the other direction. This is very consistent with the theory that these hippocampal connectivities are back projections used for memory recall, for they must be weak in this back projection direction for memory systems to operate correctly, as noted above (Rolls 2016, 2021d). Figure 4 also shows that the inferior frontal gyrus areas have weaker connectivity from these areas to other cortical areas, and this is consistent with the same hypothesis, as the inferior frontal gyrus is also implicated in memory, in this case short-term memory (Rolls 2016, 2021d). The lateral orbitofrontal cortex (47 m) effective connectivity is also interesting, as it too has weaker effective connectivity in the direction from the orbitofrontal cortex to the entorhinal, perirhinal, and parahippocampal TF cortex. Overall, what is shown in Figure 4 highlights some of the great usefulness of the approach to effective connectivity described here, by showing consistent effects across many cortical areas and systems in the directionality that is produced by the algorithm, and also how this type of analysis helps to understand and interpret in computational analyses how memory and other systems in the brain operate (Rolls 2016, 2021d).

Conclusion

In summary, this is the first quantitative assessment we know of the effective connectivity of the human hippocampal system. The connectivities of the human hippocampus that are revealed are with more cortical areas than was previously assumed, and lead to new focus on specializations in different parts of the cortical system that connect with the hippocampus, including specialization of parahippocampal TH and its VMV input regions for processing related to viewing spatial scenes (Sulpizio et al. 2020) with neurons such as spatial view cells (Georges-François et al. 1999; Rolls and Wirth 2018; Rolls 2021e), and specialization of parahippocampal TF for functions related to the ventral "object" and "face" visual system (Rolls 2012, 2021b), but also relating to anterior temporal lobe semantic systems (Bonner and Price 2013; Rolls 2021d) and language areas (Mayer et al. 2017). A highlight of the findings is that they are in the framework provided by the HCP-MMP atlas, which with its 180 cortical areas in each hemisphere, many functionally identified, allows interpretation of some of the functionality of the different connectivities described here. The effective connectivity also supports the extensive direct connections of the human hippocampal system followed with diffusion tractography which was performed in the same HCP participants, showing, for example, that the findings with tractography did not reflect incorrect following of tracts where pathways cross (Huang, Rolls, Hsu, et al. 2021b). In addition, the effective connectivity described here provides evidence not available from the tractography, about the physiological strength and direction of the connectivity. Another highlight is that these results extend considerably what is known from rodents, because humans have highly developed cortical areas including the posterior cingulate cortex and dorsal parietal and ventral visual stream areas so important in human hippocampal function, and also connections with systems in the anterior temporal lobe implicated in semantics in humans (Rolls 2021d). Another highlight is that we show that in this case important advances can be made about the connectivity of the human memory and navigation system, based on the large investments in studies designed to collect data on the human connectome

such as the HCP. Another highlight is that we emphasize the third stream of processing with the hippocampal system, the orbitofrontal/ventromedial prefrontal cortex stream (green in Fig. 5), which enables a key component of episodic memory, the reward/emotional component, to be added to the ventral stream "where" (blue color in Fig. 5) and the dorsal stream "what" (red color in Fig. 5) components for episodic memory storage and recall (Rolls 2021c).

Supplementary Material

Supplementary material can be found at *Cerebral Cortex* online.

Funding

National Key R&D Program of China (2019YFA0709502 to J.F.), 111 Project (B18015 to J.F.); Shanghai Municipal Science and Technology Major Project (2018SHZDZX01), ZJLab, and Shanghai Center for Brain Science and Brain-Inspired Technology; and National Key R&D Program of China (2018YFC1312904); Spanish national research project (PID2019-105772GB-I00 MCIU AEI to G.D.) funded by the Spanish Ministry of Science, Innovation and Universities (MCIU), State Research Agency (AEI); HBP SGA3 Human Brain Project Specific Grant Agreement 3 (945539), funded by the EU H2020 FET Flagship programme; SGR Research Support Group support (2017 SGR 1545), funded by the Catalan Agency for Management of University and Research Grants (AGAUR); Neurotwin Digital twins for model-driven non-invasive electrical brain stimulation (101017716) funded by the EU H2020 FET Proactive programme; euSNN European School of Network Neuroscience (860563) funded by the EU H2020 MSCA-ITN Innovative Training Networks; CECH The Emerging Human Brain Cluster (Id. 001-P-001682) within the framework of the European Research Development Fund Operational Program of Catalonia 2014–2020; Brain-Connects: Brain Connectivity during Stroke Recovery and Rehabilitation (id. 201725.33) funded by the Fundacio La Marato TV3; Corticity, FLAG ERA JTC 2017 (ref. PCI2018–092891) funded by the Spanish Ministry of Science, Innovation and Universities (MCIU), State Research Agency (AEI).

Notes

The neuroimaging data were provided by the Human Connectome Project, WU-Minn Consortium (Principal Investigators: David Van Essen and Kamil Ugurbil; 1U54MH091657) funded by the 16 NIH Institutes and Centers that support the NIH Blueprint for Neuroscience Research; and by the McDonnell Center for Systems Neuroscience at Washington University. Roscoe Hunter of the University of Warwick is thanked for contributing to the description in the Supplementary Material of the Hopf effective connectivity algorithm. *Conflict of Interest*: The authors have no competing interests to declare.

Ethical Permissions

No data were collected as part of the research described here. The data were from the Human Connectome Project, and the WU-Minn HCP Consortium obtained full informed consent from all participants, and research procedures and ethical guidelines were followed in accordance with the Institutional Review Boards (IRB), with details at the HCP website (http://www.humanconnectome.org/).

References

Amaral DG, Cowan WM. 1980. Subcortical afferents to the hippocampal formation in the monkey. *J Comp Neurol*. 189:573–591.

Amaral DG, Insausti R, Cowan WM. 1984. The commissural connections of the monkey hippocampal formation. *J Comp Neurol*. 224: 307–336.

Avila E, Lakshminarasimhan KJ, DeAngelis GC, Angelaki DE. 2019. Visual and vestibular selectivity for self-motion in macaque posterior parietal area 7a. *Cereb Cortex*. 29:3932–3947.

Bajaj S, Adhikari BM, Friston KJ, Dhamala M. 2016. Bridging the gap: dynamic causal modeling and granger causality analysis of resting state functional magnetic resonance imaging. *Brain Connect*. 6:652–661.

Barbas H, Blatt GJ. 1995. Topographically specific hippocampal projections target functionally distinct prefrontal areas in the rhesus monkey. *Hippocampus*. 5:511–533.

Blatt GJ, Rosene DL. 1998. Organization of direct hippocampal efferent projections to the cerebral cortex of the rhesus monkey: projections from CA1, prosubiculum, and subiculum to the temporal lobe. *J Comp Neurol*. 392:92–114.

Bonner MF, Price AR. 2013. Where is the anterior temporal lobe and what does it do? *J Neurosci*. 33:4213–4215.

Bonnici HM, Maguire EA. 2018. Two years later—revisiting autobiographical memory representations in vmPFC and hippocampus. *Neuropsychologia*. 110:159–169.

Bremmer F, Duhamel JR, Ben Hamed S, Graf W. 2000. Stages of self-motion processing in primate posterior parietal cortex. *Int Rev Neurobiol*. 44:173–198.

Bubb EJ, Kinnavane L, Aggleton JP. 2017. Hippocampal—diencephalic—cingulate networks for memory and emotion: an anatomical guide. *Brain Neurosci Adv*. 1:1–20.

Buffalo EA, Bellgowan PS, Martin A. 2006. Distinct roles for medial temporal lobe structures in memory for objects and their locations. *Learn Mem*. 13:638–643.

Burwell RD, Witter MP, Amaral DG. 1995. Perirhinal and postrhinal cortices of the rat: a review of the neuroanatomical literature and comparison with findings from the monkey brain. *Hippocampus*. 5:390–408.

Burwell RD, Amaral DG. 1998. Cortical afferents of the perirhinal, postrhinal, and entorhinal cortices of the rat. *J Comp Neurol*. 398: 179–205.

Burwell RD. 2000. The parahippocampal region: corticocortical connectivity. *Ann N Y Acad Sci*. 911:25–42.

Cheng W, Rolls ET, Gu H, Zhang J, Feng J. 2015. Autism: reduced functional connectivity between cortical areas involved in face expression, theory of mind, and the sense of self. *Brain*. 138: 1382–1393.

Clark IA, Hotchin V, Monk A, Pizzamiglio G, Liefgreen A, Maguire EA. 2019. Identifying the cognitive processes underpinning hippocampal-dependent tasks. *J Exp Psychol Gen*. 148:1861–1881.

Coalson TS, Van Essen DC, Glasser MF. 2018. The impact of traditional neuroimaging methods on the spatial localization of cortical areas. *Proc Natl Acad Sci USA*. 115:E6356–E6365.

Corkin S. 2002. What's new with the amnesic patient H.M.? *Nat Rev Neurosci*. 3:153–160.

Cullen KE. 2019. Vestibular processing during natural self-motion: implications for perception and action. *Nat Rev Neurosci*. 20: 346–363.

Deco G, Rolls ET. 2005. Attention, short-term memory, and action selection: a unifying theory. *Prog Neurobiol*. 76:236–256.

Deco G, Cabral J, Woolrich MW, Stevner ABA, van Hartevelt TJ, Kringelbach ML. 2017a. Single or multiple frequency generators in on-going brain activity: a mechanistic whole-brain model of empirical MEG data. *NeuroImage*. 152:538–550.

Deco G, Kringelbach ML, Jirsa VK, Ritter P. 2017b. The dynamics of resting fluctuations in the brain: metastability and its dynamical cortical core. *Sci Rep*. 7:3095.

Deco G, Cruzat J, Cabral J, Tagliazucchi E, Laufs H, Logothetis NK, Kringelbach ML. 2019. Awakening: predicting external stimulation to force transitions between different brain states. *Proc Natl Acad Sci*. 116:18088–18097.

DeWitt I, Rauschecker JP. 2013. Wernicke's area revisited: parallel streams and word processing. *Brain Lang*. 127:181–191.

Ding SL, Van Hoesen G, Rockland KS. 2000. Inferior parietal lobule projections to the presubiculum and neighboring ventromedial temporal cortical areas. *J Comp Neurol*. 425:510–530.

Doan TP, Lagartos-Donate MJ, Nilssen ES, Ohara S, Witter MP. 2019. Convergent projections from perirhinal and postrhinal cortices suggest a multisensory nature of lateral, but not medial, entorhinal cortex. *Cell Rep*. 29:617–627 e617.

Felleman DJ, Van Essen DC. 1991. Distributed hierarchical processing in the primate cerebral cortex. *Cereb Cortex*. 1:1–47.

Fonov V, Evans AC, Botteron K, Almli CR, McKinstry RC, Collins DL, Cooperative BD, G. 2011. Unbiased average age-appropriate atlases for pediatric studies. *NeuroImage*. 54:313–327.

Frassle S, Lomakina EI, Razi A, Friston KJ, Buhmann JM, Stephan KE. 2017. Regression DCM for fMRI. *NeuroImage*. 155:406–421.

Freyer F, Roberts JA, Becker R, Robinson PA, Ritter P, Breakspear M. 2011. Biophysical mechanisms of multistability in resting-state cortical rhythms. *J Neurosci*. 31:6353–6361.

Freyer F, Roberts JA, Ritter P, Breakspear M. 2012. A canonical model of multistability and scale-invariance in biological systems. *PLoS Comput Biol*. 8:e1002634.

Friston K. 2009. Causal modelling and brain connectivity in functional magnetic resonance imaging. *PLoS Biol*. 7:e33.

Funahashi S, Bruce CJ, Goldman-Rakic PS. 1989. Mnemonic coding of visual space in monkey dorsolateral prefrontal cortex. *J Neurophysiol*. 61:331–349.

Furtak SC, Wei SM, Agster KL, Burwell RD. 2007. Functional neuroanatomy of the parahippocampal region in the rat: the perirhinal and postrhinal cortices. *Hippocampus*. 17:709–722.

Gallivan JP, Goodale MA. 2018. The dorsal "action" pathway. *Handb Clin Neurol*. 151:449–466.

Garcia AD, Buffalo EA. 2020. Anatomy and function of the primate entorhinal cortex. *Annu Rev Vis Sci*. 6:411–432.

Ge T, Feng J, Grabenhorst F, Rolls ET. 2012. Componential granger causality, and its application to identifying the source and mechanisms of the top-down biased activation that controls attention to affective vs sensory processing. *NeuroImage*. 59: 1846–1858.

Georges-François P, Rolls ET, Robertson RG. 1999. Spatial view cells in the primate hippocampus: allocentric view not head direction or eye position or place. *Cereb Cortex*. 9:197–212.

Germann J, Petrides M. 2020. The ventral part of dorsolateral frontal area 8A regulates visual attentional selection and the dorsal part auditory attentional selection. *Neuroscience*. 441:209–216.

Gilbert SJ, Burgess PW. 2008. Executive function. *Curr Biol*. 18: R110–R114.

Gilson M, Moreno-Bote R, Ponce-Alvarez A, Ritter P, Deco G. 2016. Estimation of directed effective connectivity from fMRI functional connectivity hints at asymmetries in the cortical connectome. *PLoS Comput Biol*. 12:e1004762.

Glasser MF, Sotiropoulos SN, Wilson JA, Coalson TS, Fischl B, Andersson JL, Xu J, Jbabdi S, Webster M, Polimeni JR, et al. 2013. The minimal preprocessing pipelines for the human connectome project. *NeuroImage*. 80:105–124.

Glasser MF, Coalson TS, Robinson EC, Hacker CD, Harwell J, Yacoub E, Ugurbil K, Andersson J, Beckmann CF, Jenkinson M, et al. 2016. A multi-modal parcellation of human cerebral cortex. *Nature*. 536: 171–178.

Goldman-Rakic PS. 1996. The prefrontal landscape: implications of functional architecture for understanding human mentation and the central executive. *Philos Trans R Soc B*. 351:1445–1453.

Griffanti L, Salimi-Khorshidi G, Beckmann CF, Auerbach EJ, Douaud G, Sexton CE, Zsoldos E, Ebmeier KP, Filippini N, Mackay CE, et al. 2014. ICA-based artefact removal and accelerated fMRI acquisition for improved resting state network imaging. *NeuroImage*. 95: 232–247.

Hasselmo ME, Rolls ET, Baylis GC. 1989. The role of expression and identity in the face-selective responses of neurons in the temporal visual cortex of the monkey. *Behav Brain Res*. 32: 203–218.

Huang C-C, Rolls ET, Feng J, Lin C-P. 2021a. An extended human connectome project anatomical atlas. *Brain Struct Funct*. https://doi.org/10.1007/s00429-021-02421-6..

Huang C-C, Rolls ET, Hsu C-CH, Feng J, Lin C-P. 2021b. Extensive cortical connectivity of the human hippocampal memory system: beyond the "what" and "where" dual-stream model. *Cereb Cortex*. 31:4652–4669.

Iglesias JE, Insausti R, Lerma-Usabiaga G, Bocchetta M, Van Leemput K, Greve DN, van der Kouwe A, Alzheimer's Disease Neuroimaging I, Fischl B, Caballero-Gaudes C, et al. 2018. A probabilistic atlas of the human thalamic nuclei combining ex vivo MRI and histology. *NeuroImage*. 183:314–326.

Insausti R, Amaral DG, Cowan WM. 1987. The entorhinal cortex of the monkey: II. Cortical afferents. *J Comp Neurol*. 264:356–395.

Insausti R, Herrero MT, Witter MP. 1997. Entorhinal cortex of the rat: cytoarchitectonic subdivisions and the origin and distribution of cortical efferents. *Hippocampus*. 7:146–183.

Insausti R, Munoz M. 2001. Cortical projections of the non-entorhinal hippocampal formation in the cynomolgus monkey (*Macaca fascicularis*). *Eur J Neurosci*. 14:435–451.

Insausti R, Amaral DG. 2004. Hippocampal formation. In: Paxinos G, Mai JK, editors. *The human nervous system*. USA: Elsevier, pp. 871–914.

Kesner RP, Rolls ET. 2015. A computational theory of hippocampal function, and tests of the theory: new developments. *Neurosci Biobehav Rev*. 48:92–147.

Knierim JJ, Neunuebel JP, Deshmukh SS. 2014. Functional correlates of the lateral and medial entorhinal cortex: objects, path integration and local-global reference frames. *Philos Trans R Soc Lond Ser B Biol Sci*. 369:20130369.

Knierim JJ. 2015. The hippocampus. *Curr Biol*. 25:R1116–R1121.

Kravitz DJ, Saleem KS, Baker CI, Ungerleider LG, Mishkin M. 2013. The ventral visual pathway: an expanded neural framework for the processing of object quality. *Trends Cogn Sci*. 17: 26–49.

Kringelbach ML, McIntosh AR, Ritter P, Jirsa VK, Deco G. 2015. The rediscovery of slowness: exploring the timing of cognition. *Trends Cogn Sci*. 19:616–628.

Kringelbach ML, Deco G. 2020. Brain states and transitions: insights from computational neuroscience. *Cell Rep*. 32: 108128.

Kropff E, Carmichael JE, Moser MB, Moser EI. 2015. Speed cells in the medial entorhinal cortex. *Nature*. 523:419–424.

Kuznetsov YA. 2013. *Elements of applied bifurcation theory*. New York: Springer Science & Business Media.

Lavenex P, Amaral DG. 2000. Hippocampal-neocortical interaction: a hierarchy of associativity. *Hippocampus*. 10:420–430.

Lavenex P, Suzuki WA, Amaral DG. 2002. Perirhinal and parahippocampal cortices of the macaque monkey: projections to the neocortex. *J Comp Neurol*. 447:394–420.

Ma Q, Rolls ET, Huang C-C, Cheng W, Feng J. 2021. Extensive cortical functional connectivity of the human hippocampal memory system. *Cortex*. in press.

Maguire EA, Intraub H, Mullally SL. 2016. Scenes, spaces, and memory traces: what does the hippocampus do? *Neuroscientist*. 22: 432–439.

Markov NT, Ercsey-Ravasz M, Van Essen DC, Knoblauch K, Toroczkai Z, Kennedy H. 2013. Cortical high-density counterstream architectures. *Science*. 342:1238406.

Markov NT, Kennedy H. 2013. The importance of being hierarchical. *Curr Opin Neurobiol*. 23:187–194.

Markov NT, Ercsey-Ravasz MM, Ribeiro Gomes AR, Lamy C, Magrou L, Vezoli J, Misery P, Falchier A, Quilodran R, Gariel MA, et al. 2014a. A weighted and directed interareal connectivity matrix for macaque cerebral cortex. *Cereb Cortex*. 24:17–36.

Markov NT, Vezoli J, Chameau P, Falchier A, Quilodran R, Huissoud C, Lamy C, Misery P, Giroud P, Ullman S, et al. 2014b. Anatomy of hierarchy: feedforward and feedback pathways in macaque visual cortex. *J Comp Neurol*. 522:225–259.

Mayer KM, Macedonia M, von Kriegstein K. 2017. Recently learned foreign abstract and concrete nouns are represented in distinct cortical networks similar to the native language. *Hum Brain Mapp*. 38:4398–4412.

McCormick C, Ciaramelli E, De Luca F, Maguire EA. 2018. Comparing and contrasting the cognitive effects of hippocampal and ventromedial prefrontal cortex damage: a review of human lesion studies. *Neuroscience*. 374:295–318.

McCormick C, Barry DN, Jafarian A, Barnes GR, Maguire EA. 2020. vmPFC drives hippocampal processing during autobiographical memory recall regardless of remoteness. *Cereb Cortex*. 30: 5972–5987.

Meister MLR, Buffalo EA. 2018. Neurons in primate entorhinal cortex represent gaze position in multiple spatial reference frames. *J Neurosci*. 38:2430–2441.

Mesulam MM. 1990. Human brain cholinergic pathways. *Prog Brain Res*. 84:231–241.

Moser MB, Rowland DC, Moser EI. 2015. Place cells, grid cells, and memory. *Cold Spring Harb Perspect Biol*. 7:a021808.

Munoz M, Insausti R. 2005. Cortical efferents of the entorhinal cortex and the adjacent parahippocampal region in the monkey (*Macaca fascicularis*). *Eur J Neurosci*. 22:1368–1388.

O'Mara SM, Rolls ET, Berthoz A, Kesner RP. 1994. Neurons responding to whole-body motion in the primate hippocampus. *J Neurosci*. 14: 6511–6523.

Pandya DN, Seltzer B, Petrides M, Cipolloni PB. 2015. *Cerebral Cortex: architecture, connections, and the dual origin concept*. New York: Oxford University Press.

Pascual B, Masdeu JC, Hollenbeck M, Makris N, Insausti R, Ding SL, Dickerson BC. 2015. Large-scale brain networks of the human left temporal pole: a functional connectivity MRI study. *Cereb Cortex*. 25:680–702.

Passingham RE. 2021. *Understanding the prefrontal cortex: selective advantage, connectivity and neural operations*. Oxford: Oxford University Press.

Pauli WM, Nili AN, Tyszka JM. 2018. A high-resolution probabilistic in vivo atlas of human subcortical brain nuclei. *Sci Data*. 5: 180063.

Power JD, Barnes KA, Snyder AZ, Schlaggar BL, Petersen SE. 2012. Spurious but systematic correlations in functional connectivity MRI networks arise from subject motion. *NeuroImage*. 59: 2142–2154.

Ranganath C, Ritchey M. 2012. Two cortical systems for memory-guided behaviour. *Nat Rev Neurosci*. 13:713–726.

Razi A, Seghier ML, Zhou Y, McColgan P, Zeidman P, Park HJ, Sporns O, Rees G, Friston KJ. 2017. Large-scale DCMs for resting-state fMRI. *Netw Neurosci*. 1:222–241.

Robertson RG, Rolls ET, Georges-François P. 1998. Spatial view cells in the primate hippocampus: effects of removal of view details. *J Neurophysiol*. 79:1145–1156.

Robertson RG, Rolls ET, Georges-François P, Panzeri S. 1999. Head direction cells in the primate pre-subiculum. *Hippocampus*. 9: 206–219.

Rockland KS, Van Hoesen GW. 1999. Some temporal and parietal cortical connections converge in CA1 of the primate hippocampus. *Cereb Cortex*. 9:232–237.

Rolls ET, Robertson RG, Georges-François P. 1997. Spatial view cells in the primate hippocampus. *Eur J Neurosci*. 9:1789–1794.

Rolls ET, Treves A, Robertson RG, Georges-François P, Panzeri S. 1998. Information about spatial view in an ensemble of primate hippocampal cells. *J Neurophysiol*. 79:1797–1813.

Rolls ET, Xiang J-Z. 2005. Reward-spatial view representations and learning in the hippocampus. *J Neurosci*. 25:6167–6174.

Rolls ET, Xiang J-Z, Franco L. 2005. Object, space and object-space representations in the primate hippocampus. *J Neurophysiol*. 94: 833–844.

Rolls ET, Xiang J-Z. 2006. Spatial view cells in the primate hippocampus, and memory recall. *Rev Neurosci*. 17:175–200.

Rolls ET. 2012. Invariant visual object and face recognition: neural and computational bases, and a model. *VisNet Front Comput Neurosci*. 6(35):1–70.

Rolls ET. 2014. *Emotion and decision-making explained*. Oxford: Oxford University Press.

Rolls ET. 2016. *Cerebral Cortex: principles of operation*. Oxford: Oxford University Press.

Rolls ET. 2018a. The storage and recall of memories in the hippocampo-cortical system. *Cell Tissue Res*. 373:577–604.

Rolls ET. 2018b. *The brain, emotion, and depression*. Oxford: Oxford University Press.

Rolls ET, Wirth S. 2018. Spatial representations in the primate hippocampus, and their functions in memory and navigation. *Prog Neurobiol*. 171:90–113.

Rolls ET. 2019a. *The orbitofrontal cortex*. Oxford: Oxford University Press.

Rolls ET. 2019b. The cingulate cortex and limbic systems for emotion, action, and memory. *Brain Struct Funct*. 224:3001–3018.

Rolls ET, Mills P. 2019. The generation of time in the hippocampal memory system. *Cell Rep*. 28:1649–1658 e1646.

Rolls ET. 2020. Spatial coordinate transforms linking the allocentric hippocampal and egocentric parietal primate brain systems for memory, action in space, and navigation. *Hippocampus*. 30: 332–353.

Rolls ET, Cheng W, Feng J. 2020a. The orbitofrontal cortex: reward, emotion, and depression. *Brain Commun*. 2:fcaa196.

Rolls ET, Cheng W, Gilson M, Gong W, Deco G, Lo CZ, Yang AC, Tsai SJ, Liu ME, Lin CP, et al. 2020b. Beyond the disconnectivity hypothesis of schizophrenia. *Cereb Cortex*. 30:1213–1233.

Rolls ET. 2021a. *The hippocampus, ventromedial-prefrontal cortex, and episodic and semantic memory*.

Rolls ET. 2021b. Learning invariant object and spatial view representations in the brain using slow unsupervised learning. *Front Comput Neurosci*. 15:686239.

Rolls ET. 2021c. On pattern separation in the primate including human hippocampus. *Trends Cogn Sci*. 25:920–922.

Rolls ET. 2021d. *Brain computations: what and how*. Oxford: Oxford University Press.

Rolls ET. 2021e. Neurons including hippocampal spatial view cells, and navigation in primates including humans. *Hippocampus*. 31: 593–611.

Rosene DL, Van Hoesen GW. 1977. Hippocampal efferents reach widespread areas of cerebral cortex and amygdala in the rhesus monkey. *Science*. 198:315–317.

Saleem KS, Tanaka K. 1996. Divergent projections from the anterior inferotemporal area TE to the perirhinal and entorhinal cortices in the macaque monkey. *J Neurosci*. 16:4757–4775.

Salimi-Khorshidi G, Douaud G, Beckmann CF, Glasser MF, Griffanti L, Smith SM. 2014. Automatic denoising of functional MRI data: combining independent component analysis and hierarchical fusion of classifiers. *NeuroImage*. 90:449–468.

Satterthwaite TD, Elliott MA, Gerraty RT, Ruparel K, Loughead J, Calkins ME, Eickhoff SB, Hakonarson H, Gur RC, Gur RE, et al. 2013. An improved framework for confound regression and filtering for control of motion artifact in the preprocessing of resting-state functional connectivity data. *NeuroImage*. 64:240–256.

Seltzer B, Van Hoesen GW. 1979. A direct inferior parietal lobule projection to the presubiculum in the rhesus monkey. *Brain Res*. 179:157–161.

Shallice T, Cipolotti L. 2018. The prefrontal cortex and neurological impairments of active thought. *Annu Rev Psychol*. 69:157–180.

Sherrill KR, Chrastil ER, Ross RS, Erdem UM, Hasselmo ME, Stern CE. 2015. Functional connections between optic flow areas and navigationally responsive brain regions during goal-directed navigation. *NeuroImage*. 118:386–396.

Smith SM, Beckmann CF, Andersson J, Auerbach EJ, Bijsterbosch J, Douaud G, Duff E, Feinberg DA, Griffanti L, Harms MP, et al. 2013. Resting-state fMRI in the human connectome project. *NeuroImage*. 80:144–168.

Sulpizio V, Galati G, Fattori P, Galletti C, Pitzalis S. 2020. A common neural substrate for processing scenes and egomotion-compatible visual motion. *Brain Struct Funct*. 225:2091–2110.

Suzuki WA, Amaral DG. 1990. Cortical inputs to the CA1 field of the monkey hippocampus originate from the perirhinal and parahippocampal cortex but not from area TE. *Neurosci Lett*. 115: 43–48.

Suzuki WA, Amaral DG. 1994. Perirhinal and parahippocampal cortices of the macaque monkey - cortical afferents. *J Comp Neurol*. 350:497–533.

Treves A, Rolls ET. 1994. A computational analysis of the role of the hippocampus in memory. *Hippocampus*. 4:374–391.

Tsao A, Sugar J, Lu L, Wang C, Knierim JJ, Moser MB, Moser EI. 2018. Integrating time from experience in the lateral entorhinal cortex. *Nature*. 561:57–62.

Tsitsiklis M, Miller J, Qasim SE, Inman CS, Gross RE, Willie JT, Smith EH, Sheth SA, Schevon CA, Sperling MR, et al. 2020. Single-neuron representations of spatial targets in humans. *Curr Biol*. 30:245–253 e244.

Valdes-Sosa PA, Roebroeck A, Daunizeau J, Friston K. 2011. Effective connectivity: influence, causality and biophysical modeling. *NeuroImage*. 58:339–361.

Van Essen DC, Smith SM, Barch DM, Behrens TE, Yacoub E, Ugurbil K, Consortium WU-MH. 2013. The WU-Minn human connectome project: an overview. *NeuroImage*. 80:62–79.

Van Hoesen GW. 1982. The parahippocampal gyrus. New observations regarding its cortical connections in the monkey. *Trends Neurosci*. 5:345–350.

Winterburn JL, Pruessner JC, Chavez S, Schira MM, Lobaugh NJ, Voineskos AN, Chakravarty MM. 2013. A novel in vivo atlas of human hippocampal subfields using high-resolution 3T magnetic resonance imaging. *NeuroImage*. 74:254–265.

Wirth S, Baraduc P, Plante A, Pinede S, Duhamel JR. 2017. Gaze-informed, task-situated representation of space in primate hippocampus during virtual navigation. *PLoS Biol*. 15:e2001045.

Witter MP, Amaral DG. 2021. The entorhinal cortex of the monkey: VI. Organization of projections from the hippocampus, subiculum, presubiculum, and parasubiculum. *J Comp Neurol*. 529: 828–852.

Wurtz RH, Duffy CJ. 1992. Neuronal correlates of optic flow stimulation. *Ann N Y Acad Sci*. 656:205–219.

Xu X, Sun Y, Holmes TC, Lopez AJ. 2016. Noncanonical connections between the subiculum and hippocampal CA1. *J Comp Neurol*. 524: 3666–3673.

Zaborszky L, Hoemke L, Mohlberg H, Schleicher A, Amunts K, Zilles K. 2008. Stereotaxic probabilistic maps of the magnocellular cell groups in human basal forebrain. *NeuroImage*. 42: 1127–1141.

Zaborszky L, Gombkoto P, Varsanyi P, Gielow MR, Poe G, Role LW, Ananth M, Rajebhosale P, Talmage DA, Hasselmo ME, et al. 2018. Specific basal forebrain-cortical cholinergic circuits coordinate cognitive operations. *J Neurosci*. 38:9446–9458.

Zhong YM, Rockland KS. 2004. Connections between the anterior inferotemporal cortex (area TE) and CA1 of the hippocampus in monkey. *Exp Brain Res*. 155:311–319.